Setting frequency relays and voltage relays to protect synchronous distributed generators against islanding and abnormal frequencies and voltages

by

BOMBAY BABI

Submitted in accordance with the requirements for
the degree of

MAGISTER TECHNOLOGIAE

In the subject

ELECTRICAL ENGINEERING

at the

UNIVERSITY OF SOUTH AFRICA

SUPERVISOR: PROF S DU

NOVEMBER 2015

Abstract

This study concerns frequency relays and voltage relays applied to the protection of synchronous distributed generators operating in reactive power control mode without a frequency regulation function. The effect of active and reactive powers combination, load power factor, and reactive power imbalance are investigated for their implication for the anti-islanding setting of the frequency relay. Results reveal that the effect of these factors must be considered when setting the relay for islanding detection. For the voltage relay, results reveal that the effect of active and reactive powers combination, load power factor, and active power imbalance must be considered when setting the relay for islanding detection. The effect of multi-stage tripping on the frequency relay ability to detect island was also investigated. Results show that multi-stage tripping can improve the anti-islanding performance of the frequency relay.

Index terms: Distributed generation; embedded generation; dispersed generation; renewable energy; frequency relay; voltage relay; islanding; anti-islanding; non-detection zone;

Declaration

I declare that ***Setting frequency relays and voltage relays to protect synchronous distributed generators against islanding and abnormal frequencies and voltages*** is my own work and that all the sources that I have used or quoted have been indicated and acknowledged by means of complete references.

I further declare that I have not previously submitted this work, or part of it, for examination at Unisa for another qualification or at any other higher education institution.

Bombay Babi

Acknowledgement

I wish to express my sincere gratitude to the University of South Africa for the bursary I received. The bursary allowed me to pay for the registration fees and study fees, buy a new laptop, buy the simulation software and pay for the training on its use. Without this bursary, I wouldn't have been able to complete this dissertation.

I also express my gratitude to Mr Stuart van Zyl for his willingness to review this dissertation.

TABLE OF CONTENTS

List of abbreviations

DG: Distributed generation or distributed generator

NDZ: Non-detection zone

PF: Power factor

PUC: Point of utility connection

1. Introduction

Local generation of electricity is not a new idea. Decades ago, electricity was generated locally as users owned their own generators. With time, as more installations required electricity, the need of an economically viable way of generating and distributing electricity arose. This led to power stations and distribution networks. The very first power station was opened by Thomas Edison in 1882 at Pearl Street, New York City. There, electricity was generated by dc generators then called dynamos which were driven by steam engines. Initially a total power of 30 kW at 110 V was generated to power incandescent lights for 59 customers over a surrounding area of 2.5 square kilometres (Glover et al, 2012: 10). From there the electricity industry grew at a fast pace; a growth characterised by the reduction in the price of electricity and aided by technological accomplishments and the ingenuity of engineers. Nowadays, we are witnessing a reversion where once again, power is generated in small scale local generating plants. Distributed generation (DG) is one of the terms used to differentiate this paradigm from the conventional power generation strategy. In conventional power stations electricity is centrally generated and then transported, often over long distances to substations and then distributed to customers over a wide area. By contrast, with distributed generation, electricity is generated close to the load.

1.1 Role of distributed generation

1.1.1 Motivation for distributed generation

Renewable energy has been the focus of governments, scientists, researchers and ecologists for the past two decades and is expected to dominate governments' energy policies for the future.

The limitation of greenhouse gas emissions, the reluctance to construct new transmission networks and large generating plants, the general uncertainty in the electricity market and energy security are some of the factors behind the growth of the renewable energy industry (Lopes et al 2006: 1190-1191) (Carley, 2009) (Driesen & Belmans, 2006: 1- 2). The interest in renewable energy is evidenced by the numerous researches in the field and governments' policies, investments and international summits.

The global use of renewable energy is growing every year. The US Department of Energy (2010: 43) estimates that, including hydropower, renewable energy now

accounts for 21% of all global electricity generation. Working Group III of the Intergovernmental Panel on Climate Change (IPCC) meeting in Abu Dhabi, published on 9 May, 2011 a report in which it outlines that by the year 2050, close to 80% of the world's energy supply could be provided by renewable sources (IPCC, 2001).

There is a very close relation between renewable energy and DG because often the term distributed generation is mentioned in combination with renewable energy technologies (Ackermann et al 2001:198). Grubb (1995: I.69), notes that 60% of the renewable energy potential can be categorised as decentralised power sources.

Competition in the electricity market is another factor that promotes DG. Stoft (2002: 12) explains that competition provides stronger cost-minimising incentives than typical cost-of-service regulation and results in suppliers making many kinds of cost-saving innovations more quickly. DG is an area in which innovation may be much quicker under competition than under regulation and cogeneration is an example thereof.

1.1.2 Definition of distributed generation

Despite all the interest DG has attracted, there is not yet unanimity on what constitutes DG and different definitions and terms are used in reference thereof. For example, Anglo-American countries use the term "embedded generation", North-American countries the term "dispersed generation", and some European and Asian countries the term "decentralised generation" (Ackermann et al 2001:195).

It is commonly accepted that the prime purpose of DG is to provide active electrical power. This means that DG does not necessarily have to be capable of providing reactive power.

Disagreements concern aspects such as (Ackermann et al 2001:195):

The location of the DG

Some researchers believe that DG is generation located on the customer side of the meter while others include also the distribution network and even the transmission network.

The rating of the DG

Opinions on the maximum rating of DG vary widely.

The area supplied by the DG

Some researchers believe that all the power supplied by the DG must be consumed locally.

The technology

Often the term distributed generation is used in conjunction with renewable energy technologies, but other technologies may be used as well.

The environmental impact

DG technologies are often believed to be more environmentally friendly than conventional technologies. This may be a short-sighted opinion because it ignores the harmful emissions that occur during the other phases of development and decommissioning (exploration, manufacturing, transportation, and disposal) of the generator.

The mode of operation

There is a widespread belief that DG is locally dispatched and that it is not concerned by the rules of operation of centrally-dispatched systems (scheduling, dispatch, pool pricing). This may however depend on the applicable regulations in different countries.

The ownership

It is commonly believed that DGs must be owned by independent power producers or by customers themselves. There is however no valid reason why public electricity utilities may not own DGs.

The penetration

It is believed that DG should only provide a fraction of the local power requirement. However, with increased interest in renewable resources, the amount of DG may increase considerably.

For our purpose we shall define distributed generation in the following terms: *Distributed generation is an electrical power source connected directly to the transmission or distribution network* (Ackermann et al 2001:195).

According to this definition, only the connection point of the power source is sufficient to classify a generator as DG. All other contentious aspects are not included in the definition.

1.2 Contribution and context of the dissertation

1.2.1 Background of the research

Synchronous distributed generators (DGs) must be protected against islanded operation, particularly when the network is fitted with an auto-recloser. Islanding occurs when the DG continues to supply loads after the grid has tripped. Islanding is detrimental for the safety of the network and that of the personnel (Geidl, 2005: 12). The current industry practice is to disconnect DGs almost immediately upon the occurrence of energised islands (Geidl. 2005: 14). Many algorithms exist (Bright, 2001) (Salman, 2001) (O'Kane, 1997) (Geidl, 2005: 14 – 19) (Freitas et al, 2007) (Affonso et al, 2005) but frequency relays and voltage relays have attracted a lot of interest because of the simplicity of their control circuit and the need to avoid false tripping, a weak point of commonly used anti-islanding relays (Freitas & Xu, 2004) (Freitas et al, 2005).

The aim of this research is to study how the islanding performance characteristics of the frequency relay and voltage relay are affected by network operating parameters in order to understand how these relays should be set to detect islanding without interfering with the normal operation of the network.

1.2.2 Statement of the problem

If a frequency relay should be used to detect the islanding of a synchronous distributed generator, its anti-islanding performance characteristics must satisfy the islanding detection requirement (maximum time to detect islanding) and the frequency variation immunity requirement (range of frequency variation for which the generator is required to remain connected to the network and uphold generation) (Vieira et al, 2006: 1123 - 1125). Setting the frequency relay to satisfy the two requirements simultaneously is a challenging task. If the relay is adjusted sensitive enough to detect islanding conditions, it may disconnect the generator for frequencies lying inside the permissible operating range of the network (the range [49 Hz, 50 Hz] in this work). On the other hand, if the relay is adjusted less sensitive to satisfy the frequency variation immunity requirement, it may not detect islanding conditions timeously. Similarly, if a voltage

relay is adjusted sensitive enough to detect islanding conditions, it may disconnect the generator for voltages lying inside the permissible operating range of the network (the range [0.9 pu, 1.1 pu] in this work), and if it is adjusted less sensitive to satisfy the voltage variation immunity requirement, it may not detect islanding conditions timeously (Vieira et al, 2007: 489 - 490).

In this context, the aim of this research is to set up a guideline for setting a frequency relay to satisfy the islanding detection requirement and the frequency variation immunity requirement simultaneously. For the voltage relay, the aim is to set up a guideline for setting a voltage relay to satisfy the islanding detection requirement and the voltage variation immunity requirement.

1.2.3 Objectives of the research

This research will specifically pursue the following objectives:

(a) To investigate the effect of the following parameters on the frequency relay anti-islanding performance curve and the implication for the relay setting: island operating quadrant, load power factor (PF), and reactive power imbalance in the island (ΔQ).

(b) To investigate the effect of the following parameters on the voltage relay performance curve and the implication for the relay setting: island operating quadrant, load PF, and active power imbalance in the island (ΔP).

(c) To investigate the effect of multi-stage tripping on the frequency relay ability to detect islanding.

1.2.4 Research questions

To meet these objectives, the following questions will have to be answered.

Question 1

With respect to the frequency relay:

(a) How is the critical active power imbalance affected by the island operating quadrant?

(b) How is the critical active power imbalance affected by the load PF?

(c) How is the critical active power imbalance affected by the reactive power imbalance in the island?

(d) How is the critical active power imbalance affected by the relay frequency setting and time delay setting?

Question 2

With respect to the voltage relay:

(a) How is the critical reactive power imbalance affected by the island operating quadrant?

(b) How is the critical reactive power imbalance affected by the load PF?

(c) How is the critical reactive power imbalance affected by the active power imbalance in the island?

1.2.5 Significance of the research

This research is important to relay engineers because it sets up a guideline for adjusting the frequency relay and the voltage relay to detect islanding and abnormal frequencies and voltages without interfering with the normal operation of the network.

1.2.6 Outlining of the dissertation

An imaginary border is drawn through the connection point of the DG to the distribution line. This dissertation studies the DG side and is not interested in the substation side of the network. Our main focus is on the frequency relay and voltage relay at the connection point of the generator.

This dissertation is not concerned with the control system of the generator. This is modelled later in the study but it is for the sole purpose of facilitating the study of the relay at the connection point. Only the synchronous generator is considered here. The other types of DG technology are not of interest. Nor is the type of primary energy source (hydro, nuclear, fossil, etc.). This dissertation does not suggest new protection techniques but gives more insight on the existing ones.

The studies will be performed on a typical South African medium voltage distribution network. This means a 33 kV/ 50 Hz symmetrically loaded three-phase radial distribution network. The permissible frequency operating range of the network is [49 Hz, 51 Hz] and the permissible voltage operating range is [0.9 pu, 1.1 pu] (NERSA, 2012: 12 – 16). The studied network consists of overhead lines and transformers. It is assumed that the system is protected by only one relay, either a frequency relay or a

voltage relay, situated at the connection point of the generator. No other relay, breaker or fuse is present on the feeder.

The results of this study may be applied to similar networks.

1.2.7 Structure of the dissertation

Chapter 2 entitled literature review summarises published literature on distributed generation and materials on the synchronous generator and load representation. Chapter 3: System modelling and simulation planning lays a foundation for Chapter 4 and Chapter 5. These deal with the setting of the frequency relay and voltage relay respectively. The work concludes in Chapter 6. Here, inferences are drawn and future research is suggested. These are preceded by a general discussion and a summary of the entire dissertation.

1.3 Terminology

The meaning of most of the words used in this dissertation comply with IEEE definitions. The following is a clarification of certain words that have a particular meaning in this dissertation or that are less familiar.

Active power imbalance in the island (ΔP): The difference between the active power supplied by the generator and the active power consumed by the local load, expressed in per unit of the generator MVA rating. If the active power supplied by the generator is bigger than that consumed by the local load, the active power imbalance in the island is positive and we say that there is excess of active power in the island. The term active power imbalance is used as a short form of the term active power imbalance in the island.

Anti-islanding performance curve: For the frequency relay, the curve *islanding detection time versus active power imbalance in the island*. For the voltage relay, the curve *islanding detection time versus reactive power imbalance in the island*. The term performance curve is used as a short form of the term anti-islanding performance curve.

Anti-islanding protection: Electrical protection applied to a distributed generator to disconnect it from the main grid in the event this one trips. It is synonymous with islanding protection and loss-of-mains protection.

Frequency variation immunity requirement: Requirement for a distributed generator to remain connected to the main grid and uphold normal operation during a permissible system frequency deviation caused by a disturbance other than islanding.

Generator: A distributed generation unit. The term generator is used as a short form of the term distributed generator or distributed generation unit.

Island: A portion of the utility's distribution network energised solely by a distributed generator following the loss of the main grid.

Island operating point: Operating condition of the island before islanding that can be represented graphically with a point with an abscissa equal to the active power imbalance in the island and an ordinate equal to the reactive power imbalance in the island. The term operating point is used as a short form of the term island operating point.

Island operating quadrant: One of the four possible combinations of excess or deficit of active power imbalance in the island and excess or deficit of reactive power imbalance in the island before islanding. The term operating quadrant is used as a short form of the term island operating quadrant.

Islanding: Disconnection of the main grid during operation which results in an island. Islanding is often the result of a fault.

Local load: All loads situated on the distributed generator side of the point of utility connection.

Non-detection zone (NDZ): An operational area within which a frequency relay or a voltage relay is not able to detect an islanding condition within the maximum time defined by the applicable grid connection code. Seen differently, this is the area within the thresholds of the permissible frequency or permissible voltage operating range.

Point of utility connection (PUC): The exact point where the circuit breaker connects the distributed generation plant to the distribution network. The PUC forms the point of demarcation between the assets of the electricity utility and those of the distributed generation plant.

Power mismatch plane: A system of rectangular Cartesian coordinates where the active power imbalance in the island is represented in abscissa and the reactive power imbalance in the island is represented in ordinate.

Permissible frequency operating range: The range [49 Hz, 51 Hz]

Permissible voltage operating range: The range [0.9 pu, 1.1 pu]

Reactive power imbalance in the island (ΔQ): The difference between the reactive power supplied by the generator and the reactive power consumed by the local load, expressed in per unit of the generator MVA rating. If the reactive power supplied by the generator is bigger than that consumed by the local load, the reactive power imbalance in the island is positive and we say that there is excess of reactive power in the island. The term reactive power imbalance is used as a short form of the term reactive power imbalance in the island.

Voltage variation immunity requirement: Requirement for a distributed generator to remain connected to the main grid and uphold normal operation during permissible voltage deviations at the PUC, caused by a disturbance other than islanding.

2. Literature review

2.1 Introduction

Published literature on distributed generation covers a wide range of topics. This Chapter is mainly concerned with aspects of the operation, protection, and modelling of networks with distributed generation. Section 2.2 reviews the protection challenges that an existing network may face following the introduction of a distributed generator. Section 2.3 reviews the theory of operation and modelling of synchronous generators, and section 2.4 deals with the mathematical representation of loads for the purpose of dynamic analysis.

2.2 Protection challenges with distributed generation

2.2.1 Introduction

Conventional power systems are designed as passive networks with unidirectional power flow from the power stations at high voltage level down to the loads at medium or low voltage level. The protection system is designed based on this principle. With the introduction of a generator on the transmission or distribution line, the network becomes active and this may pose problems for the existing protection system. This chapter reviews some of the protection challenges faced by networks with distributed generation.

2.2.2 Fault current

Distributed generation may affect the amplitude, duration and direction of the fault current.

Amplitude

The amplitude of the fault current can be calculated simply by dividing the pre-fault voltage at the faulted point by the Thevenin impedance of the system at that point. With the introduction of a generator on the distribution line, the equivalent Thevenin impedance becomes smaller due to parallel paths and this will lead to increased fault currents. This situation puts protection equipment at great risk because it was not designed for this fault current.

Duration

Consider a fault at point a in Figure 2.1. The total fault current is given by $I_f = I_g + I_{dg}$. Relay R only measures a portion of the actual fault current and may not trigger within the appropriate time.

Direction

Consider a fault on bus 1 in Figure 2.1. In this case, the fault current contribution from the generator traverses the relay in reverse direction. This could pose a problem if a directional relay is used.

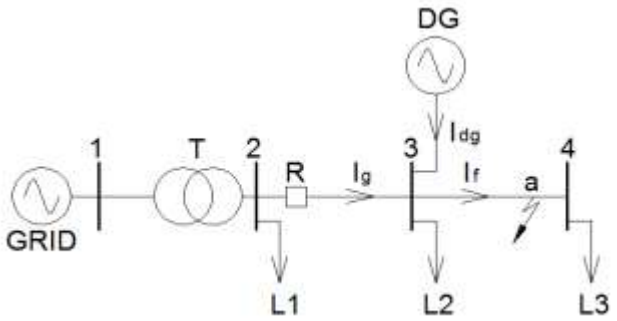

***Figure 2.1**: Distributed generator contributes to fault current (Geidl, 2005: 9)*

2.2.3 Reduced reach of impedance relays

The reach of an impedance relay is the maximum fault distance that triggers the relay in a certain impedance zone, or in a certain time due to its configuration. This maximum distance corresponds to a maximum fault impedance or a minimum fault current that is detected (Geidl, 2005: 10). Consider Figure 2.1. The voltage measured by the relay is given by (Geidl, 2005: 10):

$$V_r = I_g Z_{23} + (I_g + I_{dg}) Z_{3a} \tag{2.1}$$

Where Z_{23} is the line impedance between bus 2 and bus 3 and Z_{3a} the line impedance between bus 3 and the faulted point, a.

Now the impedance measured by the relay is

$$\frac{V_r}{I_g} = Z_{23} + Z_{3a} + \frac{I_{dg}}{I_g} Z_{3a} \tag{2.2}$$

The impedance measured by the relay is higher than the real fault impedance by an amount $\frac{I_{dg}}{I_g} Z_{3a}$ which is variable. This corresponds to an increased fault distance.

Hence, for a fault at point a, the relay will trigger in a higher grading time. For relay settings which were determined before the introduction of the generator, the fault has to be closer for the relay to trip within the originally intended zone; this corresponds to a reduced reach of the relay.

2.2.4 Reverse power flow and voltage profile

Distribution networks are designed for unidirectional power flow from the infeed down to the loads. With the introduction of a generator on the distribution line, the direction of power flow may change, particularly when the local generation exceeds the local consumption. This will affect the voltage profile.

Consider Figure 2.2 (b). The solid line shows the voltage profile before the introduction of the generator. The voltage slops from bus 1 to bus 4. The voltage gradient along the line is negative. Let's assume that a generator is connected to bus 3 and that the generator's supply is bigger than the local demand ($I_{dg} > (I_{l2} + I_{l3})$). In this case, current flows in reverse direction between bus 3 and bus 2. The voltage at bus 3 is higher than previously. The resulting voltage profile and voltage gradient are shown in dotted lines. Reverse power flow is problematic for directional relays.

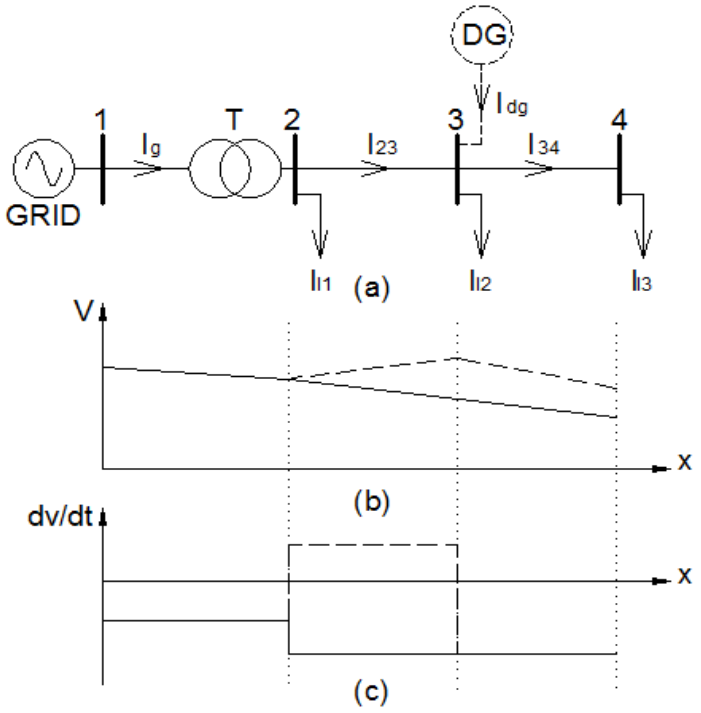

***Figure 2.2**. (a): Connection of DG to bus 3. (b): Voltage profile. (c) Voltage gradient (Geidl, 2005:11)*

Distributed generation always affects the voltage profile along the distribution line. Besides the power quality problem, this can result in the violation of voltage limits and

add additional stress to equipment. On highly loaded and weak networks, the effect of the distributed generator on the voltage profile may be a benefit.

2.2.5 Interference with tap-changing transformers

Tap changing transformers regulate the voltage on a network based on the load current. A distributed generator connected near a tap-changing transformer (for example at bus 2 in Figure 2.2 (a)) reduces the transformer load current. Consequently, the tap changing characteristics may be shifted and the voltage may not be properly regulated.

2.2.6 Islanding and automatic reclosing

Islanding occurs when the distributed generator continues to supply loads after the disconnection of the grid. Islanding can lead to serious problems. These are outlined below (Geidl, 2005: 12).

Fault arc clearing

Islanding is normally the result of a fault. When islanding occurs due to a short circuit, the fault arc may not clear even after the opening of the distribution line circuit breaker because the distributed generator will continue feeding it.

Undefined voltage magnitude

Small distributed generators are often not equipped with voltage control. When islanding occurs, the voltage in the island may fluctuate uncontrollably.

Frequency deviation

When islanding occurs, the frequency in the island may deviate considerably. Let ΣP_{dg} be the total power supplied by the generators before islanding and ΣP_l the total power consumed by the loads before islanding. Since real systems are never balanced exactly, two things will happen after islanding. If $\Sigma P_{dg} > \Sigma P_l$, the frequency in the island increases after islanding. If $\Sigma P_{dg} < \Sigma P_l$, the frequency in the island decreases after islanding.

Automatic reclosing

Two things may happen when the auto-recloser tries to reconnect the network after islanding.

(a) The fault arc may not have cleared because it was fed by the distributed generator. Hence automatic reclosing will fail.

(b) The frequency in the island may have changed during islanding due to active power imbalance and the auto-recloser will be trying to reconnect two asynchronously operating systems.

Presently, the only solution to islanding is to disconnect the distributed generator soon after the grid is lost. For that islanding has to be detected fast and reliably. Many methods exist to that effect. Some of them are reviewed in the following sections.

2.2.7 Islanding detection methods

Islanding detection methods can be classified in two groups: passive methods and active methods (Geidl, 2005: 14). In passive methods of islanding detection, the relay monitors the state of the network to decide if there is islanding. These methods are briefly discussed in the sections below.

Voltage deviation

Let ΣQ_{dg} be the total reactive power supplied by the distributed generators before islanding and ΣQ_l the total reactive power consumed by the loads before islanding. Since real systems are never balance exactly, two things will happen after islanding. If $\Sigma Q_{dg} > \Sigma Q_l$, the voltage in the island increases after islanding. If $\Sigma Q_{dg} < \Sigma Q_l$, the voltage in the island decreases after islanding. The voltage relay uses this phenomenon to detect islanding.

Frequency deviation

As explained in section 2.2.6, the frequency will deviate after islanding due to active power imbalance. The frequency relay uses this phenomenon to detect islanding.

Voltage vector shift

This method is also called phase displacement or phase jump method. Figure 2.3 (a) shows a network where part of the load is supplied by the distribution network and part by the distributed generator. The distribution network and the distributed generator are represented by their Thevenin equivalent circuits in Figure 2.3 (b). Figure 2.3 (c) shows the vector diagram for the distributed generator. After the transmission line switch opens, the load demand has to be fully met by the distributed generator. Assuming a constant load, the load current will suddenly jump after islanding and the transmission

angle, i.e. the angle between the load voltage and the generator terminal voltage, will suddenly increase. Figure 2.3 (c) and Figure 2.3 (d) show the situation in the phasor domain and in the time domain. The dotted lines correspond to the situation after islanding and the continuous lines represent parallel supply. Due to vector jump, the duration of the concerned period becomes longer. The voltage vector relay (also called vector surge relay) monitors the duration of each half cycle and trips if the threshold is reached.

Vector surge relays are susceptible to false tripping during a fault on an adjacent feeder, especially on weak networks (Freitas & Xu, 2004).

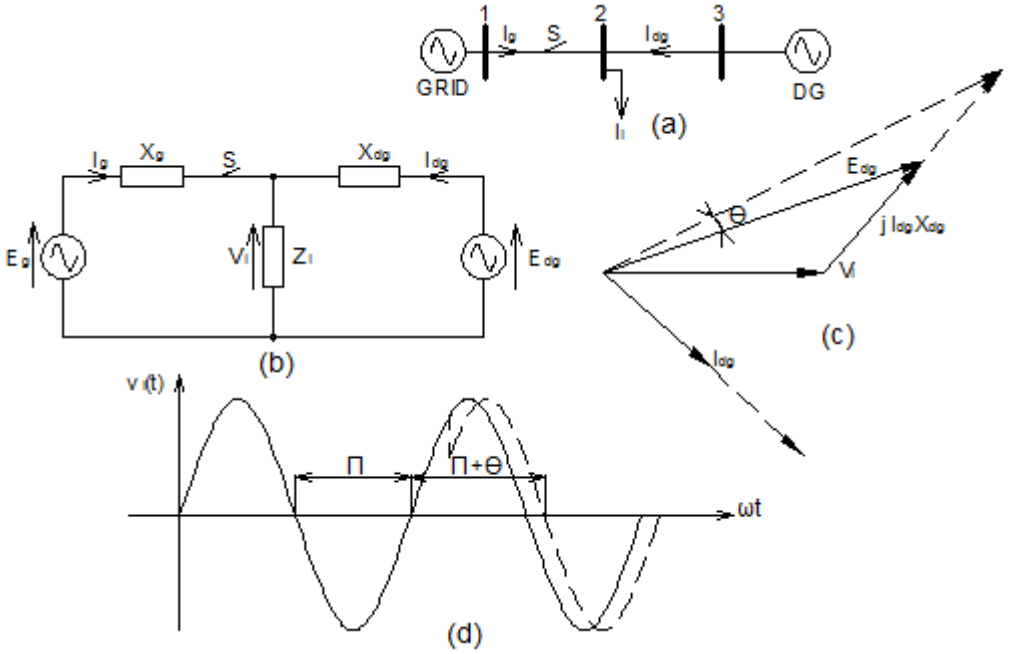

Figure 2.3. *(a): Load supplied by DG and grid. (b): Thevenin equivalent of the network. (c): Phasor domain illustration of phase jump. (d): Time domain illustration of phase jump.*

Rate of change of frequency (ROCOF)

As explained in section 2.2.6, the frequency in the island will deviate due to active power imbalance. The rate of change of frequency (df/dt) will be significantly higher during islanding. The ROCOF relay measures the rate of change of the frequency and initiates tripping when a threshold is reached.

A major problem with the ROCOF relay is false tripping due to frequency change following a loss of generation. Another reason for false tripping is phase jump caused by other faults than islanding.

Rate of change of voltage

The rate of change of voltage in large networks is normally slow. If islanding occurs, a faster rate of change of voltage occurs which can be detected by a relay after a threshold is reached (Salman et al, 2001).

Besides the passive methods of islanding detection there are also active methods. With these methods, the relay constantly communicates with the network to be informed of an islanding. These methods are very complex because they require communication between the relay and the network. Some of them are mentioned below:

Reactive error export (O'Kane & Fox, 1997)

The relay monitors the error between a fixed maximum value of reactive power that the generator is allowed to deliver and the reactive power it actually delivers. An off limits error is an indication of islanding.

System impedance monitoring (O'Kane & Fox, 1997)

The relay monitors the impedance of the system to decide whether there is islanding.

Comparison of rate of change of frequency (COROCOF) (Bright, 2001)

The COROCOF relay compares the rate of change of frequency of the generator with that of the rest of the system to decide if there is islanding.

2.2.8 Anti-islanding performance characteristics

Frequency relay

Frequency relays can be used to protect synchronous distributed generators against islanding. For that purpose, the relay anti-islanding performance characteristics must satisfy the islanding detection requirement (maximum time to detect islanding) and the frequency variation immunity requirement (range of permissible frequencies for which the generator is required to remain connected to the network and uphold normal generation) (IEEE, 2003: 9).

When employed for anti-islanding protection, frequency relays are triggered by the frequency variation in the island after the disconnection of the grid. If prior to islanding the active power supplied by the generator was bigger than the active power consumed by the local load (excess of active power in the island), the frequency in the island will

rise upon the occurrence of islanding and trigger the relay when the value reaches the relay overfrequency setting. Likewise, if prior to islanding the active power supplied by the generator was smaller than the active power consumed by the local load (deficit of active power in the island), the frequency in the island will fall upon the occurrence of islanding and trigger the relay when the value reaches the relay underfrequency setting.

Adjusting a frequency relay to satisfy the islanding detection requirement and the frequency variation immunity requirement is a challenging task. If the relay is adjusted sensitive enough to detect islanding conditions, it may disconnect the generator for frequencies lying inside the normal operating range of the network (the range [49 Hz, 51 Hz] in this paper). On the other hand, if the relay is adjusted less sensitive to satisfy the frequency variation immunity requirement, it may not detect islanding conditions timeously (Vieira et al, 2006: 1123).

This problem is solved by determining the critical active power imbalance of the relay in the islanding detection time versus active power imbalance graph. If a frequency relay must be adjusted to detect islanding effectively without violating the frequency variation immunity requirement, its performance curve must present an active power imbalance bigger than the critical active power imbalance (considering absolute values) (Vieira et al, 2006: 1124).

The anti-islanding performance characteristics of the frequency relay can be defined in a three-dimensional Cartesian coordinates system (ΔP, ΔQ, t) as shown in Figures 2.4, 2.5 and 2.6. In Figure 2.4, the islanding detection time (t) axis is not seen because it is perpendicular to the plane of the paper. ΔP and ΔQ are respectively the active and reactive power imbalances in the island at islanding. A positive value of ΔP or ΔQ represents excess power. As shown in Figure 2.4, any particular situation of power imbalance in the island, can be represented by a unique point called the *island operating point* (point A for example) in the (ΔP, ΔQ) plane called the *power mismatch plane* (Vieira et al, 2008: 594).

ΔP axis and ΔQ axis define four quadrants (Q1 to Q4) in the power mismatch plane in which the following operating conditions prevail:

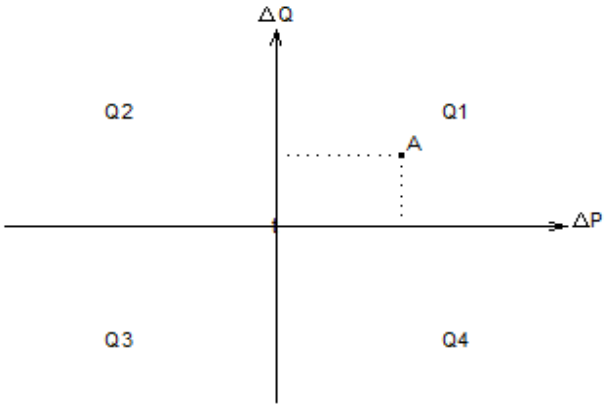

***Figure 2.4**: Power mismatch plane with islanding detection time axis perpendicular to the plane of this paper*

Q1: excess of active and reactive powers

Q2: deficit of active power and excess of reactive power

Q3: deficit of active and reactive powers

Q4: excess of active power and deficit of reactive power

Point B in Figure 2.5 is the *relay operating point*. Its position is defined by the island operating point and by the islanding detection time.

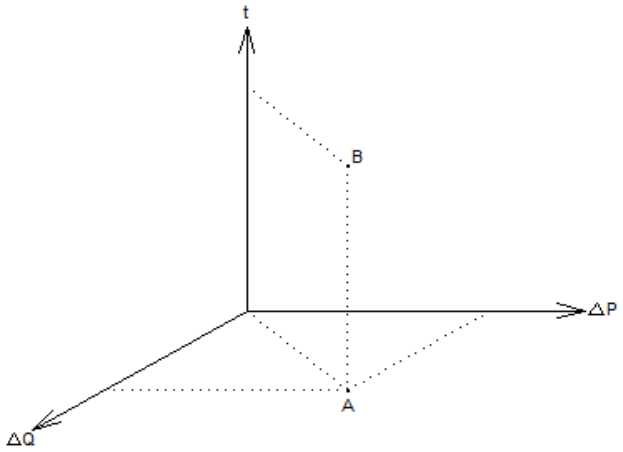

***Figure 2.5**: Power mismatch plane and islanding detection time axis*

The reactive power imbalance axis cannot be seen in Figure 2.6 because it is perpendicular to the plane of the paper. In reactive power control mode generators operate at constant reactive power output (Jenkins et al, 2000: 103). Thus island operating points can be seen as points on the ΔP axis and the frequency relay operating point can be seen as a point in the (ΔP, t) graph.

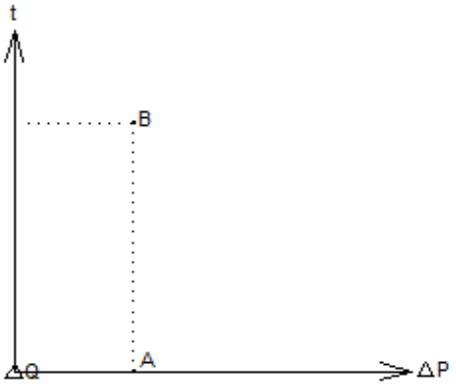

***Figure 2.6**: Power mismatch plane with ΔQ axis perpendicular to the plane of this paper*

In this way, the sets of active power imbalance and islanding detection time at constant reactive power imbalance can be used to plot the performance curve of the frequency relay in the (ΔP, t) plane, literally omitting the ΔQ axis.

Figure 2.7 is an example of a frequency relay performance curve. It was plotted using repeated simulations. The active power imbalance values in this figure are in pu referred to the generator MVA rating. The curve was plotted for a frequency of 51 Hz and a time delay of 0 ms.

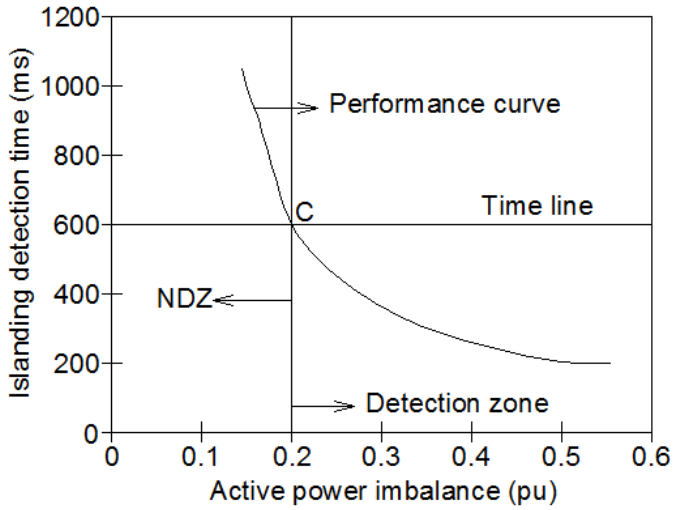

***Figure 2.7**: Anti-islanding performance curve of a frequency relay*

If we define an islanding detection time of 600 ms for example, we can obtain an operating point (point C) on the performance curve. The value of active power imbalance at this point (0.2 pu) is called the *critical active power imbalance*. This is the smallest value of active power imbalance for which islanding is detected timeously. The area on the left of point C is the non-detection zone (NDZ) of the frequency relay. In this area, islanding conditions are not detected timeously. This area corresponds to

the normal operation of the network. No performance curve must lie inside this area since this will cause the relay to trip the generator between 50 Hz and 51 Hz. That is why the frequency relay performance curve must present an active power imbalance bigger than the critical active power imbalance to satisfy the islanding detection requirement and the frequency variation immunity requirement.

The islanding detection time of a frequency relay may be calculated directly by applying equation (2.3) (Vieira et al, 2006: 1125 – 1126). This equation gives an estimate of the islanding detection time and allows the protection engineer to adjust the instantaneous and time delay settings readily, thus avoiding time consuming simulations.

$$t = \frac{2H\Delta f}{f_o \Delta P_o^{\left(\frac{1}{0.8}\right)}} + t_d \qquad (2.3)$$

In this equation, t is the islanding detection time (in seconds), H the inertia constant of the synchronous generator (in pu), f_o, the rated frequency of the network (in Hz) and ΔP_o, the active power imbalance at the instant of islanding (in pu). Δf and t_d are relay settings with Δf being the frequency setting (in Hz) and t_d the time delay setting (in seconds).

Equation (2.3) does not account for the effect of reactive power imbalance on the islanding detection time. For accurate results, simulations should be run, considering the reactive power imbalance in the island.

Voltage relay

The voltage relay can protect a synchronous distributed generator against islanding. To accomplish this task reliably, the relay must fulfil two requirements: the islanding detection requirement (maximum time to detect islanding) and the voltage variation immunity requirement (range of permissible voltages for which the generator should remain connected to the network and uphold generation) (the range [0.9 pu, 1.1 pu] in this work).

When employed for islanding protection, voltage relays are triggered by the voltage variation in the island after the disconnection of the grid. If at the time the grid trips the reactive power supplied by the generator is bigger than the reactive power consumed by the local load (excess of reactive power in the island), the voltage in the island will rise and trigger the relay when the value reaches the relay overvoltage setting. Likewise, if at the time the grid trips the reactive power supplied by the generator is

smaller than the reactive power consumed by the local load (deficit of reactive power in the island), the voltage in the island will fall and trigger the relay when the value reaches the relay undervoltage setting.

If a voltage relay must be adjusted to detect islanding without violating the voltage variation immunity requirement, its performance curve must present a reactive power imbalance bigger than the critical reactive power imbalance (Vieira et al, 2007: 489 – 490).

Let's turn the three-dimensional Cartesian coordinates system of Figure 2.5 so that the active power imbalance axis is perpendicular to the plane of this paper (see Figure 2.8).

If we consider that the active power imbalance is constant (This assumption is valid because DGs generally operate at constant active power output (Jenkins et al, 2000: 136)), island operating points can be seen as points on the ΔQ axis and the voltage relay operating point can be seen as a point in the (ΔQ, t) graph. Thus the sets of reactive power imbalance and islanding detection time at constant active power imbalance can be used to plot the performance curve of the voltage relay in the (ΔQ, t) plane, omitting the ΔP axis altogether.

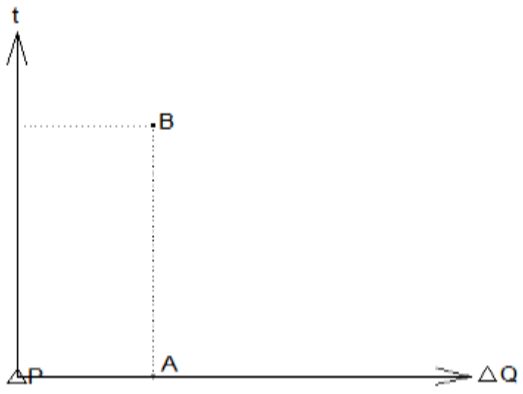

***Figure 2.8**: Power mismatch plane with ΔP axis perpendicular to the plane of the paper*

Figure 2.9 is an example of a voltage relay performance curve. The reactive power imbalance values in this figure are in pu referred to the MVA rating of the generator. The curve was plotted for a voltage of 1.1 pu and a time delay of 0 ms.

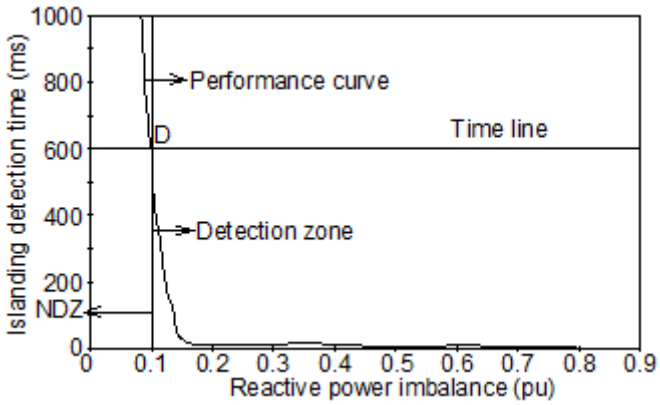

***Figure 2.9**: Anti-islanding performance curve of a voltage relay*

If we define an islanding detection time of 600 ms for example, point D can be determined on the performance curve. The value of reactive power imbalance at this point (0.1 pu) is called the *critical reactive power imbalance*. This is the smallest value of reactive power imbalance for which islanding is detected timeously. The area on the left of point D is the non-detection zone of the voltage relay. In this area, islanding conditions are not detected timeously. This area corresponds to the normal operation of the network. The voltage relay must not present performance curves in this area as this will cause the relay to trip the generator between 1.0 pu and 1.1 pu. This is why the performance curve of a voltage relay must present a reactive power bigger than the critical reactive power imbalance to detect islanding without violating the voltage variation immunity requirement.

2.2.9 Frequency variation immunity requirement

Synchronous DGs that are not equipped with a frequency control function are required to withstand frequency deviations at the PUC while reducing their active power output as little as possible. Hence they operate as a constant power source.

Figure 2.10 shows the characteristic minimum DG disconnection time as a function of network frequency, recommended by NERSA (2012: 13) for DGs connected to the South African network. We note for example that when the frequency on the network is higher than 51.5 Hz for longer than 4 seconds or less than 47 Hz for longer than 200 ms, the DG is disconnected from the network. However, the DG may not be disconnected when the frequency fluctuates between 49 Hz and 51 Hz. This range constitutes the permissible frequency operating range defined in section 1.3.

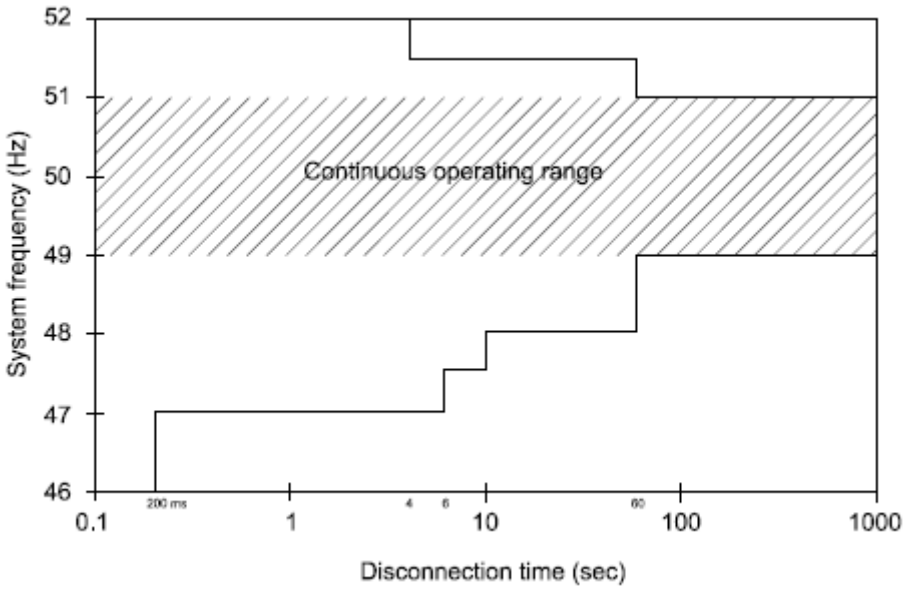

***Figure 2.10**: Characteristic minimum DG disconnection time versus system frequency (NERSA, 2012:13)*

2.2.10 Voltage variation immunity requirement

Figure 2.11 shows the characteristic minimum DG disconnection time as a function of network voltage (NERSA, 2012: 16). We can see for example that when the network voltage is higher than 1.2 pu for longer than 2 seconds or zero pu for longer than 0.15 second the generator is disconnected from the network. However, when the network voltage fluctuates between 0.9 pu and 1.1 pu, the DG may not be disconnected. This range constitutes the permissible voltage operating range defined in section 1.3.

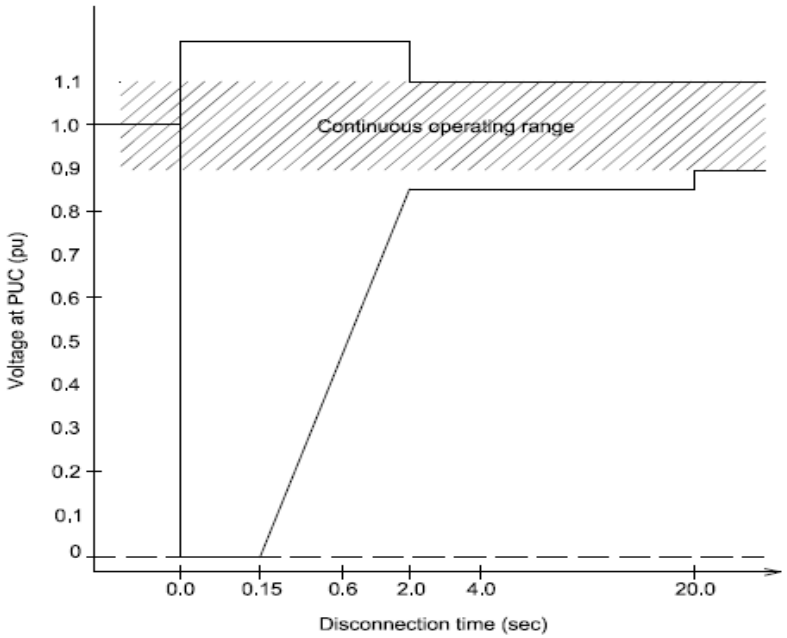

***Figure 2.11**: Characteristic minimum DG disconnection time versus voltage at PUC (NERSA, 2012:16)*

2.3. Aspects of synchronous machines operation and modelling

2.3.1 Introduction

The synchronous machine is a versatile machine. When driven by a turbine, it operates as a generator and converts mechanical energy into electrical energy. When connected to a voltage source, it operates as a motor and converts electrical energy into mechanical energy. Here we are mainly concerned with synchronous generators, in particular synchronous generators connected to an infinite bus. The main area of focus is the control and modelling of such generators.

2.3.2 Description of synchronous machines

The synchronous machine has two main parts: the stator also called armature, and the rotor. The stator is a hollow cylinder with slots cut longitudinally along the inner surface. Inside these slots are windings that carry the current supplied to a load in the case of a generator or the current received from the voltage source in the case of a motor. The rotor is mounted on a shaft and rotates inside the stator. The rotor can be of one of two possible designs: cylindrical rotor or salient pole rotor. The rotor carries the field winding which is supplied by a dc source termed the exciter. The magneto motive force (mmf) produced by the field winding combines with that produced by the armature windings to create a magnetic flux in the air gap between the rotor and the stator. This flux is responsible for the voltage induced in the armature windings and the electromagnetic torque on the shaft of the machine. If the machine is a motor, the electromagnetic torque on the shaft drives the mechanical load coupled to the shaft. If the machine is a generator, the electromagnetic torque on the shaft opposes the torque on the prime mover.

2.3.3 Equivalent circuits of the synchronous machine

Figure 2.12 shows the equivalent circuits of the synchronous machine. In Figure 2.12 (a), the machine is operating as a generator and supplies current to the load. The internal voltage E_a forces current through the load and is termed electromotive force (emf). In Figure 2.12 (b), the machine is operating as a motor and receives current from the voltage source. The internal voltage E_a opposes the voltage and is termed counter-electromotive force (cemf).

The combined quantity $\omega\,(L_s + M_s)$ in the two circuits has the dimensions of a reactance and is called *synchronous reactance* (X_d) of the machine. The *synchronous impedance*

(Z_d) of the machine includes both the armature resistance and the synchronous reactance.

$$Z_d = R + j\,X_d \tag{2.4}$$

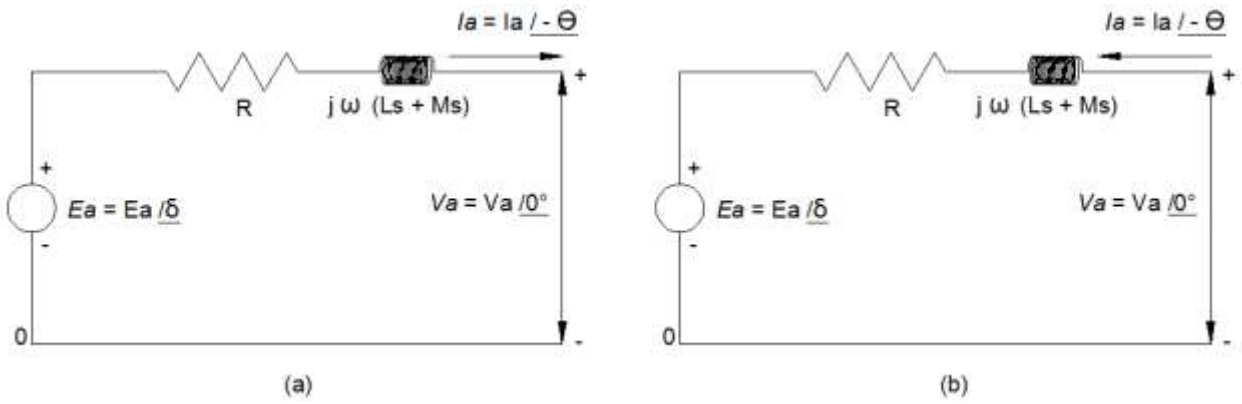

***Figure 2.12**: Equivalent circuits of a synchronous machine. (a): generator. (b): motor*

2.3.4 Phasor diagrams

Using Figure 2.12 (a) we can develop the following equation for a synchronous generator:

$$E_a = V_a + I_a\,R + j\,I_a\,X_d \tag{2.5}$$

This equation is represented with the phasor diagram of Figure 2.13 (a) for a lagging armature current. Figure 2.13 (b) for the synchronous motor leads to equation (2.6) and to the phasor diagram of Figure 2.13 (b).

$$V_a = E_a + I_a\,R + j\,I_a\,X_d \tag{2.6}$$

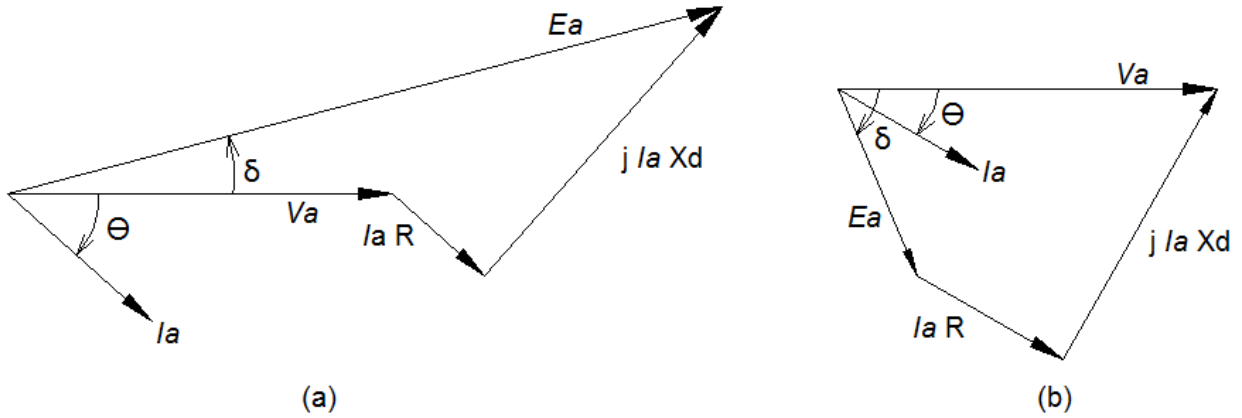

***Figure 2.13**: Phasor diagrams of a synchronous machine operating with a lagging current. (a): generator. (b): motor*

2.3.5 Reactive and active power controls

When a synchronous machine is connected to an infinite bus its speed is fixed and cannot be altered because it is imposed by the system frequency. The terminal voltage is also fixed and cannot be changed because it is imposed by the system voltage. The only two control variables available are the excitation current and the shaft torque.

For simplicity, let's neglect the comparatively small armature resistance and let's call the armature voltage V_t (for terminal voltage) rather than V_a. Figure 2.13 (a) is redrawn as Figure 2.14 (a) taking into account this adjustments.

The complex power supplied by the generator to the infinite bus is given by

$$S = \mathrm{P} + \mathrm{j}\,\mathrm{Q} = V_t I_a^* = \mathrm{V_t}\,\mathrm{I_a}\,(\cos\theta + \mathrm{j}\sin\theta) \tag{2.7}$$

Equating real and imaginary parts, we have:

$$\mathrm{P} = \mathrm{V_t}\,\mathrm{I_a}\cos\theta \tag{2.8}$$

$$\mathrm{Q} = \mathrm{V_t}\,\mathrm{I_a}\sin\theta \tag{2.9}$$

Q is positive for lagging power factors and negative for leading power factors.

Reactive power control

It is clear from equations (2.8) and (2.9) that if we want to vary the reactive power in such a way that the active power is not affected, $\mathrm{I_a}\cos\theta$ must remain constant. We can see in Figure 2.14 (a) that this can be achieved by varying the machine's emf E_a. As the field current is varied, Ea moves along line BD in such a way that $\mathrm{I_a}\cos\theta$ is always constant.

Normal excitation is the condition when $\mathrm{E_a}\cos\delta = \mathrm{V_t}$. The machine is said to be overexcited or underexcited depending on whether $\mathrm{E_a}\cos\delta > \mathrm{V_t}$ or $\mathrm{E_a}\cos\delta < \mathrm{V_t}$. In Figure 2.14 (a), the generator is overexcited and supplies reactive power to the network. From the system point of view, the machine operates as a capacitor. In Figure 2.14 (b), the machine is underexcited and absorbs reactive power. From the system point of view, it operates as an inductor.

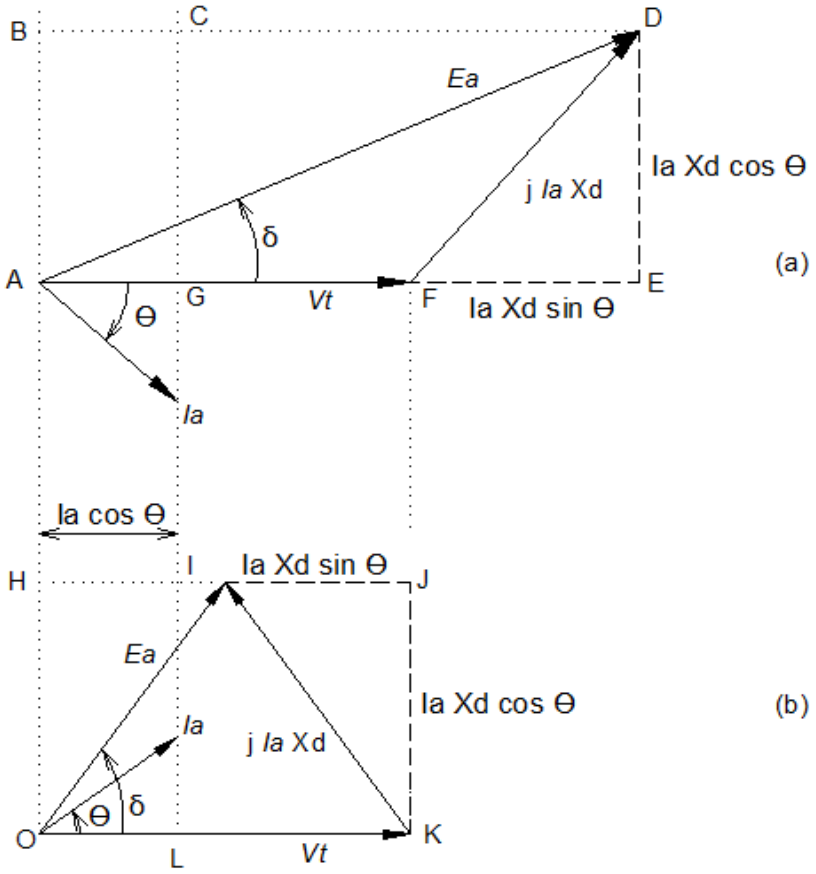

***Figure 2.14**: Reactive power control. (a): Overexcited generator delivering reactive power to the system. (b): Underexcited generator receiving reactive power from the system (Grainger & Stevenson, 1994: 106).*

Figure 2.15 shows the phasor diagrams of an overexcited and an underexcited synchronous motor. The machine in Figure 2.15 (a) is overexcited and absorbs leading current. From the point of view of the network where it is connected, it behaves like a capacitor supplying reactive power. The machine in Figure 2.15 (b) is underexcited and absorbs lagging current. This machine behaves like an inductor when viewed from the network from which it absorbs reactive power.

We can then conclude from the study of Figure 2.14 and Figure 2.15 that overexcited generators and motors supply reactive power to the system and underexcited generators and motors absorb reactive power from the system.

Active power control

The active power of the generator is increased by allowing more water or more steam through the valves of the turbine. As more water or more steam comes in, the speed of the rotor starts to increase and angle δ starts to increase too. This can be seen if vector E_a is turned counter clockwise in Figures 2.14 (a) and 2.14 (b). If the excitation

is kept constant, the quantity $I_a \cos \theta$ increases proportionally. A machine with a bigger $I_a \cos \theta$ supplies more power and exerts a bigger counter torque on the shaft of the prime mover. Finally, balance is reached with a bigger prime mover torque and a speed corresponding to the frequency of the network

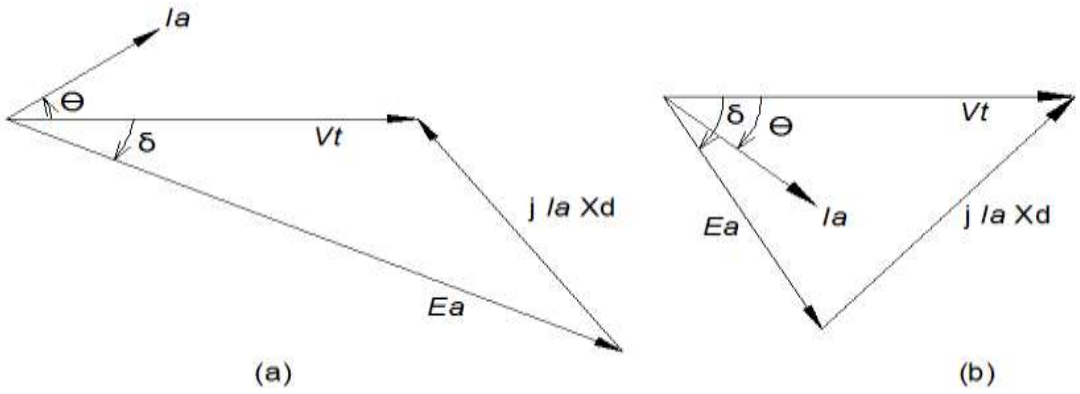

Figure 2.15*: Phasor diagrams of a synchronous motor. (a): Overexcited motor supplying reactive power to the system. (b): Underexcited motor absorbing reactive power from the system.*

2.3.6 The two-axis synchronous machine model

The theory and equations presented above for the cylindrical rotor machine are accurate for steady-state performance analysis only. For transient analysis, the two-axis model of the machine is used. The theory and equations for the two-axis model are developed considering a salient pole rotor because it has unequal air gaps along the direct axis and the quadrature axis between the poles. The air gap along the direct axis is narrower than the air gap along the quadrature axis.

The stator of a cylindrical rotor machine and that of the salient pole machine are exactly the same. However, because of the unequal air gaps in the salient pole machine, the self and mutual inductances of the armature coils are not constant like those of the cylindrical rotor machine but rather vary with the rotor position. For both machines the field winding has a constant self- inductance and a mutual inductance with the armature winding that is a cosine function of the rotor position.

In brief, except for the field winding self-inductance, all the inductances of a salient pole machine vary with the rotor position. This makes the manipulation of the equations of a salient pole machine more difficult than those of a cylindrical rotor machine. Luckily, the equations of the salient pole machine can be expressed in a simple form

by transforming the a, b, and c variables of the stator into corresponding sets of new variables called the direct-axis, quadrature-axis and zero-sequence quantities which are distinguished by the subscripts d, q, and 0 respectively. For example armature currents i_a, i_b, and i_c can be transformed into currents i_d, i_q, and i_o called the direct-axis current, quadrature-axis current and zero-sequence current respectively. The transformation is made through the application of a matrix $\mathbf{P}$ called Park's transformation. Park's matrix which is given below has a particular algebraic property called orthogonality. This means that the transpose of the matrix is the same as its inverse. Orthogonality ensures that the power delivered by phases a, b, and c is conserved after the transformation.

$$\mathbf{P} = \sqrt{\frac{2}{3}}\begin{bmatrix} \cos\theta d & \cos(\theta d - 120°) & \cos(\theta d - 240°) \\ \sin\theta d & \sin(\theta d - 120°) & \sin(\theta d - 240°) \\ \frac{1}{\sqrt{2}} & \frac{1}{\sqrt{2}} & \frac{1}{\sqrt{2}} \end{bmatrix} \tag{2.10}$$

The currents, voltages, and flux linkages of phases a, b, and c are transformed to the d, q, and 0 variables as follows:

$$\begin{bmatrix} id \\ iq \\ io \end{bmatrix} = \mathbf{P}\begin{bmatrix} ia \\ ib \\ ic \end{bmatrix} \qquad \begin{bmatrix} vd \\ vq \\ vo \end{bmatrix} = \mathbf{P}\begin{bmatrix} va \\ vb \\ vc \end{bmatrix} \qquad \begin{bmatrix} \lambda d \\ \lambda q \\ \lambda o \end{bmatrix} = \mathbf{P}\begin{bmatrix} \lambda a \\ \lambda b \\ \lambda c \end{bmatrix} \tag{2.11}$$

Park's transformation defines a set of currents, voltages, and flux linkages for three fictitious windings: the d-winding, the q-winding, and the 0-winding. The d-winding and the q-winding rotate in synchronism with the field winding and have a constant mutual inductance with this winding and with any other winding that may exist in the machine. The 0-winding is stationary.

2.3.7 Standard parameters

When there is a disturbance on the network or in the loading of the synchronous machine, the rotor swings. The swinging of the rotor causes currents to be induced in its windings. Some of these currents decay very fast and they are called *subtransient currents*. Some decay slowly and they are called *transient currents*. There are also *steady-state currents* that are sustained by the machine during normal operation after the rotor has reached dynamic equilibrium.

Reactances that determine subtransient currents are called *subtransient reactances*. Reactances that determine transient currents are called *transient reactances*, and those that determine the steady-state currents are called *synchronous reactances*.

The reactance affects the magnitude of the current, but the rate of decay of the current depends on the time constant of the circuit. We define *subtransient* and *transient time constants* as those time constants that determine the rate of decay of the subtransient and transient currents.

These time constants together with the reactances defined above constitute the *standard parameters* of a synchronous machine which are used to characterise the machine for dynamic performance. The standard parameters of a synchronous machine are calculated for the fundamental frequency currents. They can be accurately calculated from the two-axis operational parameters of the machine. The interested reader may consult Kundur (1994: 144) for these calculations. Table 2.1 gives typical values of standard parameters for hydraulic and thermal units.

***Table 2.1**: Typical values of standard parameters of synchronous machines (Kundur, 1994: 153)*

Parameter		Hydraulic units	Thermal units
Synchronous reactance	X_d	0.6- 1.5	1.0 – 3.2
	X_q	0.4 – 1.0	1.0 – 2.3
Transient reactance	X'_d	0.2 – 0.5	0.15 – 0.4
	X'_q	-	0.3 – 1.0
Subtransient reactance	X''_d	0.15 – 0.35	0.12 – 0.25
	X''_q	0.2 – 0.45	0.12 – 0.25
Transient open circuit time constant	T'_{do}	1.5 – 9.0	3.0 – 10.0
	T''_{qo}	-	0.5 – 2.0
Subtransient open circuit time constant	T''_{do}	0.01 – 0.05	0.02 – 0.05
	T''_{qo}	0.01 – 0.09	0.02 – 0.05
Stator leakage reactance	X_l	0.1 – 0.2	0.1 – 0.2
Stator resistance	R_a	0.002 – 0.02	0.0015 – 0.005

Notes: Reactance values are in per unit of the machine rated values. Time constants are in seconds

2.3.8 Rotor dynamics and the swing equation

When a synchronous machine is operating in steady-state and a sudden change in the operating quantities of the system or machine occurs, we say that the machine has undergone a disturbance. A machine is operating in steady-state if all the measured or calculated quantities describing the operating condition can be considered constant for the purpose of analysis. Disturbances can be small or big. Big disturbances are often

caused by generation loss, load loss, line switching, or line faults. An adjustment in the parameters of the excitation system for example would cause a small disturbance.

A power system is steady-state stable for a given operating point if, following a small disturbance it returns to the same operating point. However, if following a big disturbance, it returns to a different stable operating point, we say that the system is transiently stable.

Often transient stability studies are carried out for the first swing which lasts one second. If the system is found to be stable during the first swing, it is considered to be transiently stable. First swing transient stability studies use a simplified generator having a transient emf E' behind a transient synchronous reactance X'_d. In these studies, excitation systems and speed governors are not represented. Multiswing stability studies extend over longer periods. The effects of the synchronous generator control units are represented because they can affect its dynamic behaviour.

The purpose of all stability studies is to determine whether or not the speed of the synchronous machine's rotor will return to synchronous speed after the disturbance. The equation governing the rotor dynamics during a disturbance is called the swing equation and it is given below as equation (2.13) (Grainger & Stevenson, 1994: 701).

To simplify calculations, three fundamental assumptions are made in all stability studies (Grainger & Stevenson, 1994: 697):

(a) Only the fundamental component of currents and voltages is considered. The dc offset and harmonic components are neglected.

(b) Symmetrical components are used to represent unbalanced faults.

(c) The effect of rotor speed swings on the emf is neglected.

$$\frac{2\,H}{\omega_s}\,\frac{d^2\,\delta}{d\,t^2} = Pa = Pm - Pe \qquad (2.12)$$

The parameters in this equation have the following meanings: H is the inertia constant of the rotor in MJ/MVA. ω_s is the synchronous speed in rad/s. δ is the angular displacement of the rotor, in electrical degrees, from a synchronously rotating reference axis. t is the time in seconds. P_m is the mechanical power input to the machine. P_e is the electrical power output, and P_a the accelerating power which

accounts for any imbalance between P_m and P_e. P_m, P_e, and P_a are expressed in pu on the same base as H.

2.3.9 Excitation system modelling

The mathematical model of the excitation system is very important for the assessment of the desired performance requirements. It must be compatible with the purpose of the study being carried out. Figure 2.16 presents the mathematical model of the IEEE type AC1A excitation system (IEEE, 2005: 10 – 11).

This exciter represents a field-controlled alternator-rectifier exciter. The main exciter is an alternator with non-controlled rectifiers. The exciter does not employ self excitation and the voltage regulator power is taken from a source that is not affected by external transients. The characteristic of the rectifier in the exciter output imposes a lower limit of zero on the exciter output voltage.

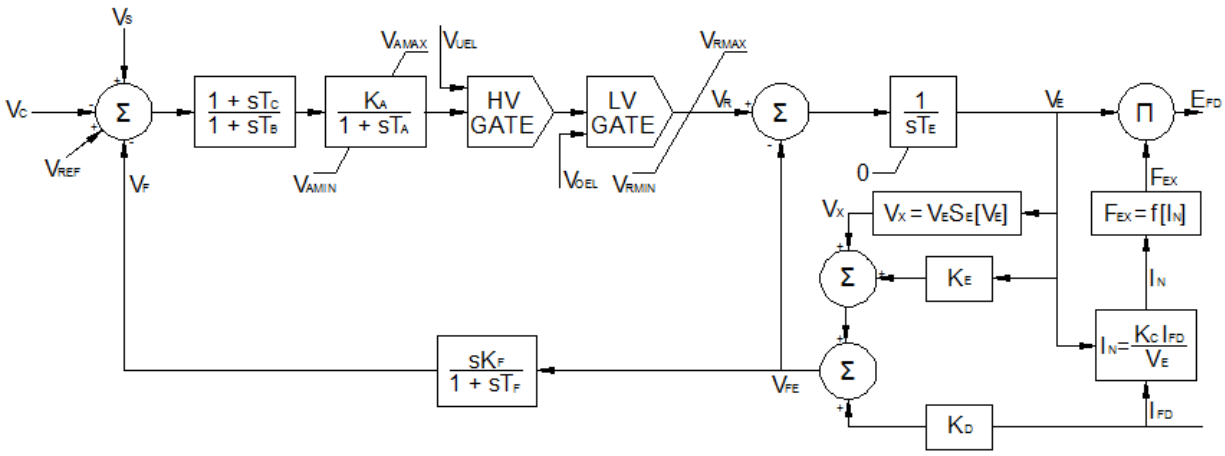

***Figure 2.16**: Mathematical model of IEEE type AC1A excitation system (IEEE, 2005: 11)*

The parameters of Figure 2.16 have the following meaning:

E_{FD}: Exciter output voltage [pu]

F_{EX}: Rectifier loading factor, a function of IN [pu]

I_{FD}: Synchronous machine field current [pu]

I_N: Normalised exciter load current [pu]

K_A: Regulator gain [pu]

K_C: Field circuit commutating reactance [pu]

K_D: Exciter constant related to field [pu]

K_E: Exciter constant related to field [pu]

K_F: Rate feedback gain [pu]

S_E [V_{E1}]: Saturation at V_{E1} [pu]

S_E [V_{E2}]: Saturation at V_{E2} [pu]

T_A: Regulator time constant [s]

T_B: Lag time constant [s]

T_C: Lead time constant [s]

T_E: Exciter time constant [pu]

T_F: Rate feedback time constant [pu]

V_{AMAX}, V_{AMIN}: Maximum and minimum regulator internal voltages [pu]

V_C: Output of terminal voltage transducer and load compensation elements [pu]

V_{E1}: Exciter voltage for S_{E1} [pu]

V_{E2}: Exciter voltage for S_E2 [pu]

V_F: Excitation system stabiliser output [pu]

V_{FE}: Signal proportional to exciter field current [pu]

V_{OEL}: Over-excitation limiter input [pu]

V_R: Voltage regulator output [pu]

V_{REF}: Voltage regulator reference (determined to satisfy initial conditions) [pu]

V_{RMAX}, V_{RMIN}: Maximum and minimum regulator outputs [pu]

V_S: Combined power stabiliser and possibly discontinuous control output after any limits of switching, as summed with terminal voltage reference signals [pu]

V_{UEL}: Under-excitation limiter input [pu]

V_X: Signal proportional to exciter saturation [pu]

***Table 2.2**: Sample data for a type AC1A excitation system (IEEE, 2005: 67)*

Parameter	Value	Parameter	Value	Parameter	Value
T_R	0	K_F	0.03	V_{AMIN}	-14.5
R_C	0	T_F	1.0	V_{RMAX}	6.03
X_C	0	K_E	1.0	V_{RMIN}	-5.43
K_A	400	T_E	0.8	$S_E[V_{E1}]$	0.10
T_A	0.02	K_D	0.38	V_{E1}	4.18
T_B	0	K_C	0.2	$S_E[V_{E2}]$	0.03
T_C	0	V_{AMAX}	14.5	V_{E2}	3.14

2.4. Aspects of load modelling for dynamic analysis

2.4.1 Introduction

This section reviews the modelling of power system loads for dynamic simulation purposes.

The power system engineer bases decisions concerning system modification in large part on the results of power flow and stability simulation analysis. For reliable results, it is therefore important that all system components be modelled accurately in the simulation programme.

The modelling of rotating machines, transmission and distribution lines and transformers is well understood but the modelling of loads remains an area of great uncertainty because of the following factors (IEEE, 1993: 472):

(a) Large number of diverse load components.

(b) Inability of the electricity utility to access loads situated on customer premises.

(c) Changing load composition with time, weather condition and season.

(d) Lack of precise information on the composition of the load.

(e) Uncertainty regarding the characteristics of many load components, e.g. the variation of the power absorbed by the load with the variation of voltage or frequency.

To improve load modelling, a number of load models have been devised. These will be reviewed in this section.

2.4.2 Definition of terms

The terms in this section comply with IEEE definitions (IEEE, 1993: 472 – 475).

Load

The term load may have several meanings in power system engineering, including:

(a) A device connected to a power system that consumes power.

(b) The total power (active and/ or reactive) consumed by all devices connected to a power system.

(c) A portion of the power system that is viewed as a single device consuming power.

(d) The power supplied by a generator or generating plant.

In this work, “load” should be understood as defined in (c) above. This means that “load” includes not only the connected load device but all ancillary equipment that are necessary for the correct functioning of the load device and its electrical protection and the protection of users and maintenance personnel.

Accurate load representation should therefore account for the effect of the load itself and the effect of all ancillary equipment.

Load characteristic

The term load characteristic refers to the set of all parameters that characterise the behaviour of a specific load, like for example, power factor, variation of active or reactive power with voltage or frequency, etc.

Load model

A load model is a mathematical equation that represents the relationship between the load terminal voltage and the power consumed by the load.

Static load model

A static load model is a load model that represents the active and reactive powers consumed by the load at any instant of time as functions of the voltage magnitude and frequency at the same instant.

Static load models are used for the representation of physically static loads, e.g. a resistive load and as an approximation for physically dynamic loads, e.g. motor-driven loads.

Dynamic load model

A dynamic load model is a load model that represents the active and reactive powers consumed by the load at any instant of time as functions of the voltage magnitude and frequency at past instants of time and, usually, including the present instant.

Dynamic load models often make use of difference and differential equations.

Constant impedance load model

It is a static load model for which the active and reactive powers consumed vary proportionally with the square of the terminal voltage magnitude.

Constant current load model

It is a static load model for which the active and reactive powers consumed vary proportionally with the terminal voltage magnitude.

Constant power load model

It is a static load model for which the active and reactive powers consumed do not vary with the variation of the terminal voltage magnitude.

Constant power loads such as motors and electronic devices do not maintain this characteristic below some voltage (typically 80 to 90%) (IEEE 1993: 473). Because of that, many computer programmes provide for changing constant power and constant current loads to constant impedance loads or tripping the load outside a specified voltage range.

2.4.3 Basic static load models

Polynomial load model

A polynomial load model represents the relationship between the power and the voltage magnitude as a polynomial equation, usually in the following form (IEEE, 1993:473):

$$P = P_o \left[a_1 \left(\frac{V}{V_o} \right)^2 + a_2 \left(\frac{V}{V_o} \right) + a_3 \right] \quad (2.13)$$

$$Q = Q_o \left[a_4 \left(\frac{V}{V_o} \right)^2 + a_5 \left(\frac{V}{V_o} \right) + a_6 \right] \quad (2.14)$$

The parameters of this model are the coefficients a_1 to a_6 and the power factor of the load. This model is sometimes referred to as the ZIP model because the two polynomials consist of constant impedance (Z), constant current (I) and constant power (P) monomials.

When this model or similar ones are used to represent a load device, V_o, P_o and Q_o are the rated terminal voltage and rated active and reactive powers. However, if the models represent a bus load, V_o, P_o and Q_o should be taken as the values at the initial system operating condition for the study.

Exponential load model

An exponential load model represents the relationship between the power and the voltage magnitude as an exponential equation, usually in the following form (IEEE, 1993:474):

$$P = P_o \left(\frac{V}{V_o} \right)^{NP} \quad (2.15)$$

$$Q = Q_o \left(\frac{V}{V_o} \right)^{NQ} \quad (2.16)$$

The parameters of this model are the power factor of the load and the exponents NP and NQ. By setting these exponents to 0, 1 or 2, this model may represent constant power, constant current or constant impedance loads. Other exponents may be suitable for other types of loads. The meanings of NP and NQ are:

$NP = dP/dV =$ voltage index for real power

$NQ = dQ/dV =$ voltage index for reactive power

Frequency-dependent load model

A frequency-dependent load model is a static load model that accounts for the frequency dependence of the load. This is achieved by multiplying either the polynomial or the exponential load models by a factor of the following form (IEEE, 1993:474):

$$[1 + K_F(f - f_o)] \tag{2.17}$$

where f is the frequency of the bus voltage, f_o, the load rated frequency and K_F the frequency sensitivity parameter of the model. A frequency dependent exponential load model will take the form

$$P = P_o \left(\frac{V}{V_o}\right)^{NP} (1 + K_{PF} df) \tag{2.18}$$

$$Q = Q_o \left(\frac{V}{V_o}\right)^{NQ} \left(1 + K_{QF} df\right) \tag{2.19}$$

The meanings of K_{PF} and K_{QF} in these two equations are:

$K_{PF} = dP/df =$ frequency index for real power

$K_{QF} = dQ/df =$ frequency index for reactive power

3. System modelling and simulation planning

3.1 Introduction

Nowadays there are numerous softwares for simulating power systems. A number of factors influence the choice of a software, including financial considerations, the objective of the study and the end users of the results. The accuracy and the detail of the results are very important to consider. These are anticipated during the research planning and design stage. One factor between different softwares is the form in which the results are presented. It is desirable that these are readily usable.

Power systems simulation softwares may be broadly classified as dynamical simulation softwares or steady-state simulation softwares. Dynamical simulation softwares perform a time domain analysis of the system model and display the results as a graph in addition to a listing of instantaneous values of the output variables. Steady-state simulation softwares perform a steady-state analysis of the network model and display the results as rms values or vectors (magnitude and phase angle).

Regardless of the software used, the need for accurate and reliable results remains unquestionable. To achieve these, the network data used as input data and the data for network components modelling must be accurate. This is a serious problem with simulation since accurate data may not always be available and the researcher may have to resort to approximations or omissions. The general results hence obtained may be acceptable if sufficiently small errors are maintained.

3.2 The simulation software

The research questions of section 1.2.4 seek to understand how different parameters affect the correlation between the islanding detection time and the power imbalance. To answer these questions, the study should be carried out in the time domain. Hence, a dynamical simulation software is needed. PSCAD (Power Systems Computer-Aided Design) was chosen. PSCAD is a time domain simulation software for studying the transient behaviour of electrical, electromagnetic, and electromechanical systems. It allows the user to schematically represent a circuit, run a simulation, analyse the results, and manage the data in an integrated graphical environment. EMTDC (Electromagnetic Transients including DC) which is the processor represents and solves the differential equations of the circuit represented in PSCAD in the time domain.

3.3 Description of the test system

The test system used in this work is schematically represented in Figure 3.1. It comprises a 30 MVA synchronous distributed generator (DG) with a rated reactive power of 18 MVAR operating in reactive power control mode. The generator is connected via two transformers to a 132 kV/ 50 Hz subtransmission system with a short-circuit level of 1500 MVA represented by a constant voltage source (CVS). A relay (either a frequency relay or a voltage relay) protects the generator against islanded operation and abnormal system frequencies or voltages at the point of utility connection (PUC). It acts on circuit breaker Bkr. S is a switch.

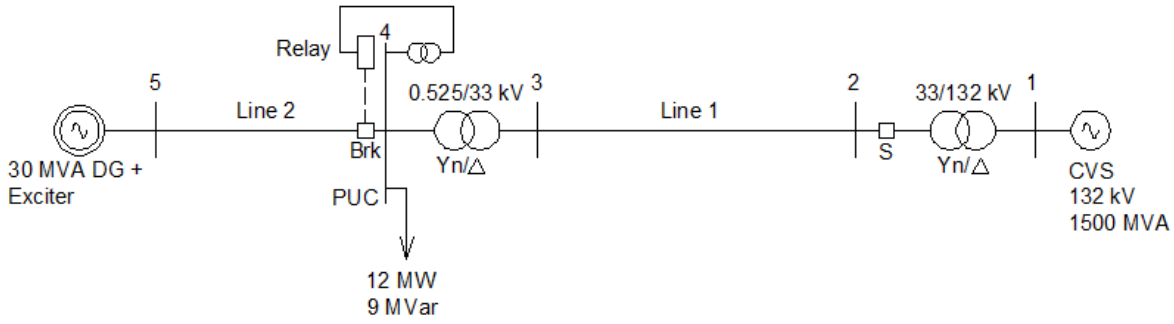

***Figure 3.1**: Schematic of the test system*

3.4 System components model and data

3.4.1 Constant voltage source data

The data for the constant voltage source is presented in Table 3.1. The values of resistance and inductance were calculated by assuming a PF angle of 89°.

***Table 3.1**: Constant voltage source (CVS) data*

Nominal voltage (kV)	132
Short circuit power (MVA)	1500
Resistance (Ω)	0.17
Inductance (mH)	3.1

3.4.2 Frequency relay model

The frequency relay will be modelled as shown in Figure 3.2 to fulfil the characteristic of Figure 2.10. The relay checks whether the network frequency is above or below the thresholds and gives the tripping order to breaker Brk. The relay is inhibited when the

distributed generator output voltage (V_{dg}) is lower than 0.6 pu to avoid that the breaker trips at start up.

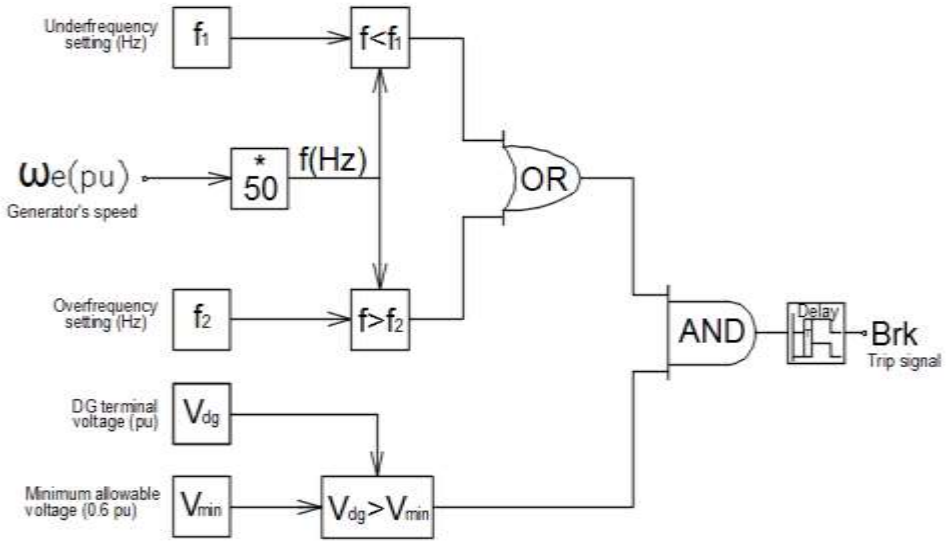

***Figure 3.2**: Frequency relay model*

The input parameters to this model are the underfrequency setting (f_1), the overfrequency setting (f_2), the generator terminal voltage (V_{dg}), the generator speed (ω_e), the time delay setting (t_d), and the minimum allowable voltage (V_{min}). V_{min} is set equal to 0.6 pu for simulation purposes. The generator terminal voltage is measured at the PUC while the generator speed is measured on the shaft. The values of f_1, f_2, and t_d may be found in the characteristic of Figure 2.10. f_1 = 49 Hz, f_2 = 51 Hz, and the range 49 Hz $\leq$ f $\leq$ 51 Hz is the permissible frequency operating range of the network or the NDZ of the frequency relay. The values of t_d are summarised in Table 3.2.

***Table 3.2**: Time delay settings of the frequency relay model*

System frequency	t_d (sec)
f > 51.5 Hz	4
51 Hz < f $\leq$ 51.5 Hz	60
49 Hz $\leq$ f $\leq$ 51 Hz	Infinitely long
48 Hz $\leq$ f < 49 Hz	60
47.5 Hz $\leq$ f < 48 Hz	10
47 Hz $\leq$ f < 47.5 Hz	6
f < 47 Hz	0.2

3.4.3 Voltage relay model

The voltage relay will be modelled as shown in Figure 3.3 to fulfil the characteristic of Figure 2.11. The relay checks whether the distributed generator terminal voltage (V_{dg}) is above or below the threshold and gives the tripping order to breaker Brk. The relay is inhibited until the system reaches steady-state stability. This is to avoid that the breaker opens and closes endlessly due to transient voltages at start up.

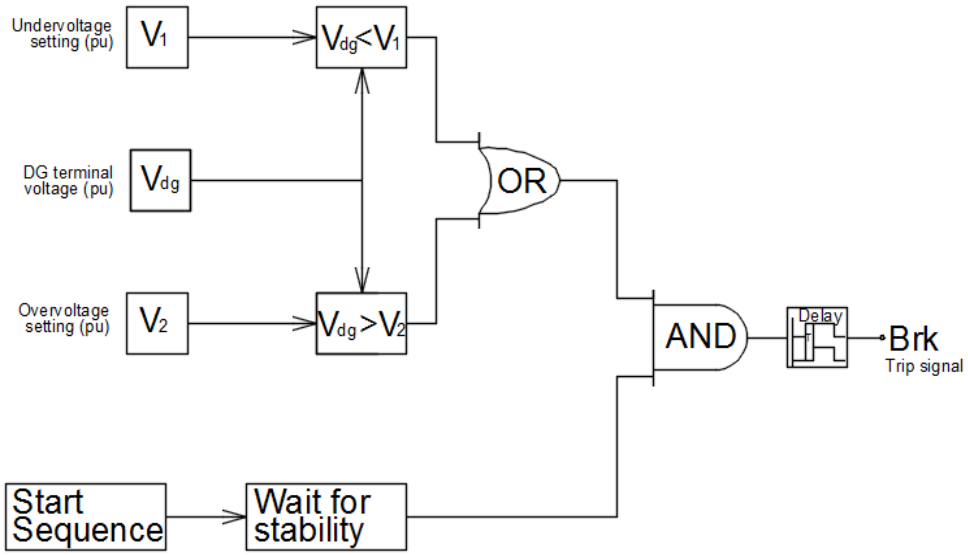

***Figure 3.3**: Voltage relay model*

The input parameters to this model are the generator terminal voltage (V_{dg}), which is measured at the PUC, the undervoltage setting (V_1), the overvoltage setting (V_2), and the time delay setting (t_d). The values of these three parameters are found in Figure 2.11. V_1 = 0.9 pu, V_2 = 1.1 pu, and the range 0.9 pu ≤ V ≤ 1.1 pu defines the permissible voltage operating range of the network or the NDZ of the voltage relay. The values of t_d are summarised in Table 3.3

***Table 3.3**: Time delay settings of the voltage relay model*

Voltage at PUC	t_d (sec)
V > 1.1 pu	2
0.9 pu ≤ V ≤ 1.1 pu	Infinitely long
0.85 pu ≤ V < 0.9 pu	20
0 pu ≤ V < 0.85 pu	2.174 V + 0.15

3.4.4 Lines and transformers models

Lines are represented as lumped RL impedances while transformers are represented with their equivalent T circuits. The data are presented in Tables 3.4 and 3.5.

***Table 3.4**: Lines data*

	Line 1	Line 2
Resistance (mΩ)	36.2	0.362
Inductance (mH)	1.24	0.0124

***Table 3.5**: Transformers data*

	Transformer	
	132/ 33 kV	33/ 0.525 kV
Nominal power (MVA)	50	50
Primary winding	Δ	Δ
Primary voltage (kV)	132	33
Secondary winding	Y_n	Y_n
Secondary voltage (kV)	33	0.525
Resistance (pu)	0	0
Inductance (pu)	0.1	0.1

3.4.5 Excitation system model

The exciter is an IEEE type AC1A exciter, the data of which is given in Table 3.6 (IEEE, 2005: 67).

The simulations that will be carried out in this work require that the generator's emf is immune to system disturbances to avoid that such disturbances induce noise that might unintentionally affect the relay's anti-islanding performance. It is for this reason that an IEEE type AC1A exciter was chosen. This exciter does not employ self excitation and its voltage regulator is powered by an external source that is not affected by system transients (see section 2.3.8).

***Table 3.6**: Exciter data*

T_R (s)	0	K_F (pu)	0.03	V_{AMIN} (pu)	-
R_C (pu)	0	T_F (s)	1.0	V_{RMAX} (pu)	6.03
X_C (pu)	0	K_E (pu)	1.0	V_{RMIN} (pu)	-
K_A (pu)	400	T_E (s)	0.8	$S_E[V_{E1}]$ (pu)	0.10
T_A (s)	0.02	K_D (pu)	0.38	V_{E1} (pu)	4.18
T_B (s)	0	K_C (pu)	0.2	$S_E[V_{E2}]$ (pu)	0.03
T_C (s)	0	V_{AMAX} (pu)	14.5	V_{E2} (pu)	3.14

3.4.6 Governor model

The active power output of the generator is considered constant because the simulation time (1500 ms) is very short. Hence, the speed governor is not modeled.

3.4.7 Synchronous generator model

The generator is a steam turbogenerator. It will be represented with the two-axis model. The data is presented in Table 3.7.

***Table 3.7**: Synchronous generator data*

Pair of poles	2
Nominal power (MVA)	30
Nominal voltage (V)	525
Inertia constant, H(s)	2.0
Rated angular speed, ω_o (rad/s)	314.159
X_d(pu)	1.79
X_d'(pu)	0.169
X_d"(pu)	0.135
X_q(pu)	1.71
X_q'(pu)	0.228
X_q"(pu)	0.2
T'_{do}(s)	4.3
$T"_{do}$(s)	0.032
T'_{qo}(s)	0.85
$T"_{qo}$(s)	0.05
Armature resistance (pu)	0.002
Potier reactance, X_p(pu)	0.13

3.4.8 Load model

Islanding is hardest to detect with constant impedance loads (Vieira et al, 2008: 596 - 598) (Vieira et al, 2005: 1661). For this reason loads will be modelled as non-frequency

dependent constant impedance loads (IEEE, 1993: 473). Hence, dP/dV = dQ/dV = 2 and dP/df = dQ/df = 0 (see section 2.4.3). The load data is presented in Table 3.8.

***Table 3.8**: Load data*

dP/dV	2
dQ/dV	2
dP/df	0
dQ/df	0
Frequency (Hz)	50
Line rms voltage (kV)	0.525
Rated three-phase real power (MW)	12
Rated three-phase reactive power (MVAR)	9

3.5 Methods of validation of simulation results

The simulation results obtained in this work will be validated against calculation results or corresponding data of another relay (which we call reference relay) operating in similar conditions. The intention is to verify that simulation results are reasonable. The calculated value of an output variable or the corresponding data of a reference relay will be considered as the expected value of that variable. Then the simulation results will be compared against it to see how close they come. Two statistical measures of central tendency will be used to decide how close to the expected result the simulated results are. These are the standard deviation (σ) and the absolute deviation (D_i).

3.5.1 Standard deviation

The standard deviation (σ) of a sample $x_1 \ldots x_n$ of n data points having a mean value or expected value $\bar{x}$ is given by equation (3.1):

$$\sigma = \sqrt{\frac{1}{n-1}\sum_{i=1}^{n}(x_i - \bar{x})^2} \qquad (3.1)$$

A standard deviation close to zero indicates that the data points tend to be very close to the mean or the expected value of the data set, while a high value of standard deviation indicates that the data points are spread out over a wider range of values.

In science researchers often report the standard deviation of experimental data. Only data points that fall farther than 2σ from $\bar{x}$ are considered a serious deviation. Deviations within 2 σ of $\bar{x}$ are seen as caused by normal random error or variation in the measurements.

3.5.2 Absolute deviation

The absolute deviation (D_i) of a data point x_i of a sample $x_1 \ldots x_n$ of n data points having a mean value or expected value $\bar{x}$ is given by equation (3.2):

$$D_i = |x_i - \bar{x}| \tag{3.2}$$

An absolute deviation close to zero indicates that the data point is very close to the mean or the expected value of the data set, while a high value of absolute deviation indicates that the data point is far from the mean value or the expected value of the data set.

4. Setting the frequency relay

4.1 Introduction

Frequency relays employed for the islanding detection of a synchronous generator must be set so as not to interfere with the normal operation of the network. For that to be possible, the relay's anti-islanding performance curve must present an active power imbalance bigger than the critical active power imbalance. For a given islanding detection time, the critical active power imbalance will be affected by many operating parameters including island operating quadrant, load PF and reactive power imbalance in the island. The objective of this chapter is to investigate how these parameters affect the anti-islanding performance curve (and hence the critical active power imbalance) of the frequency relay in order to understand how to safely set the relay when these parameters are changing. The chapter also investigates the effect of multi-stage setting on the relay's ability to detect islanding.

4.2 Simulation procedure

The simulations will use the test system of Figure 4.1.

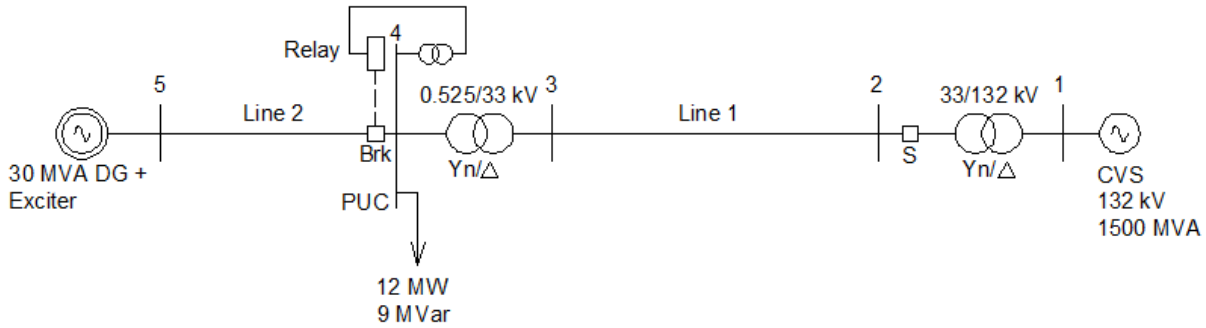

***Figure 4.1**: Schematic of the test system*

Repeated simulations will be performed to determine relay operating points which will then be used to plot the performance curve. The procedure to obtain the relay operating points is described as follows: The active power imbalance in the island is gradually varied from 0 to 1.0 pu in Q1 and Q4 and from 0 to – 1.0 pu in Q2 and Q3 by varying the generator active power output. For each active power imbalance value, an islanding is simulated by opening switch S. Then the pairs of active power imbalance at bus 4 and relay pickup time are used to project the relay operating points.

4.3 Flowchart of the simulation process

Three groups of simulations (impact of the operating quadrant on the relay performance, impact of load PF on the relay performance, and impact of reactive power imbalance on the relay performance) are carried out in the following sections, the ultimate objective of each group of simulations being the determination of conditions in which islanding is hardest to detect. These conditions form the most pessimistic cases of islanding detection and inform the setting of the relay. The flowchart of Figure 4.2 pictures the interaction between these groups. Another group of simulations (impact of multi-stage tripping on the relay performance) is run independently and is not represented in the flowchart.

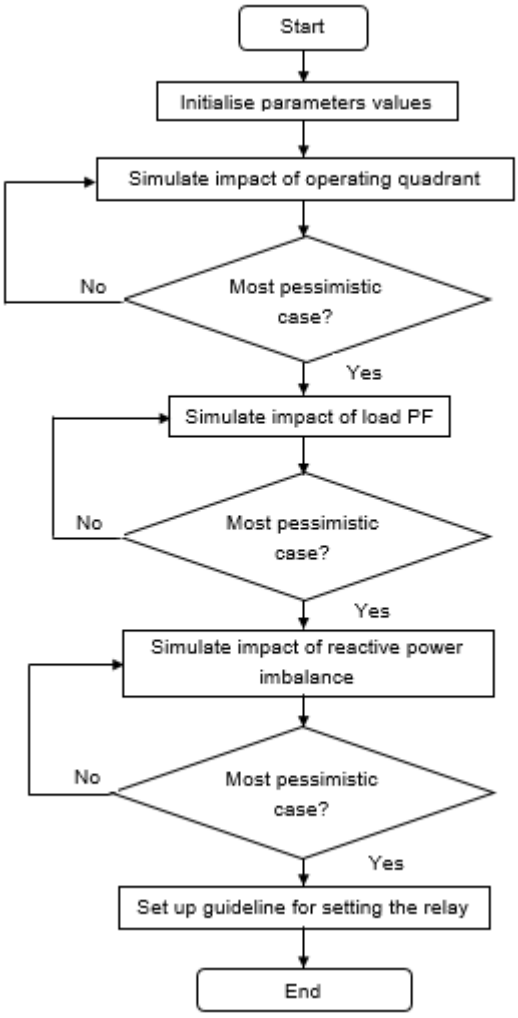

***Figure 4.2**: Flowchart of the simulation process to study the anti-islanding performance of the frequency relay and set up a guideline for adjusting the relay*

4.4 Impact of operating quadrant on the relay performance

4.4.1 Simulation results

Figure 4.3 presents the results of the simulations to study the effect of the operating quadrant on the relay anti-islanding performance. The simulations were carried out on a load of 12 MVA considering PFs of unity, 0.8 lagging, and 0.9 leading. The reactive power imbalance in the island was maintained constant at 0.1 pu in Q1 and Q2 and – 0.1 pu in Q3 and Q4. The relay frequency and time delay settings were fixed at 51 Hz/ 0 ms in Q1 and Q4 and 49 Hz/ 0 ms in Q2 and Q3.

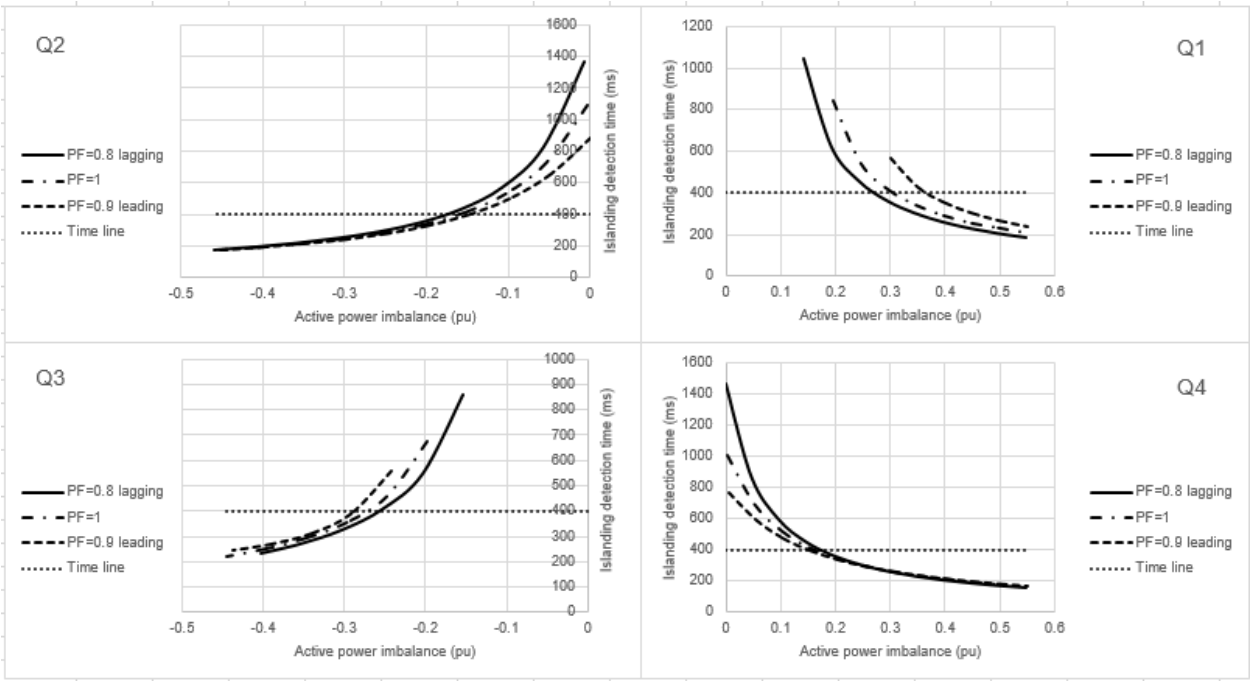

Figure 4.3*: Impact of operating quadrant on the performance curve of the frequency relay*

4.4.2 Validation of the simulation results

The anti-islanding performance curve of a frequency relay can be plotted using equation (2.11) which is rewritten here as equation (4.1) for convenience.

$$t = \frac{2H\Delta f}{f_o \Delta P_o{}^{(\frac{1}{0.8})}} + t_d \qquad (4.1)$$

The curve labelled *Formula* in Figure 4.4 was plotted from this equation. The values assigned to the different parameters of the equation are: H = 2.0 s, Δf = 1 Hz, t_d = 0 ms, and f_o = 50 Hz.

If we consider the calculated value of active power imbalance ($\overline{\Delta P}$) for a given islanding detection time (t) as the expected value, then the sample standard deviation (σ) of a sample $\Delta P_i \ldots \Delta P_n$ consisting of active power imbalances determined by simulation for the same islanding detection time can be calculated in accordance with equation (3.1) as follows:

$$\sigma = \sqrt{\frac{1}{n-1} \sum_{i=1}^{n} (\Delta P_i - \overline{\Delta P})^2} \qquad (4.2)$$

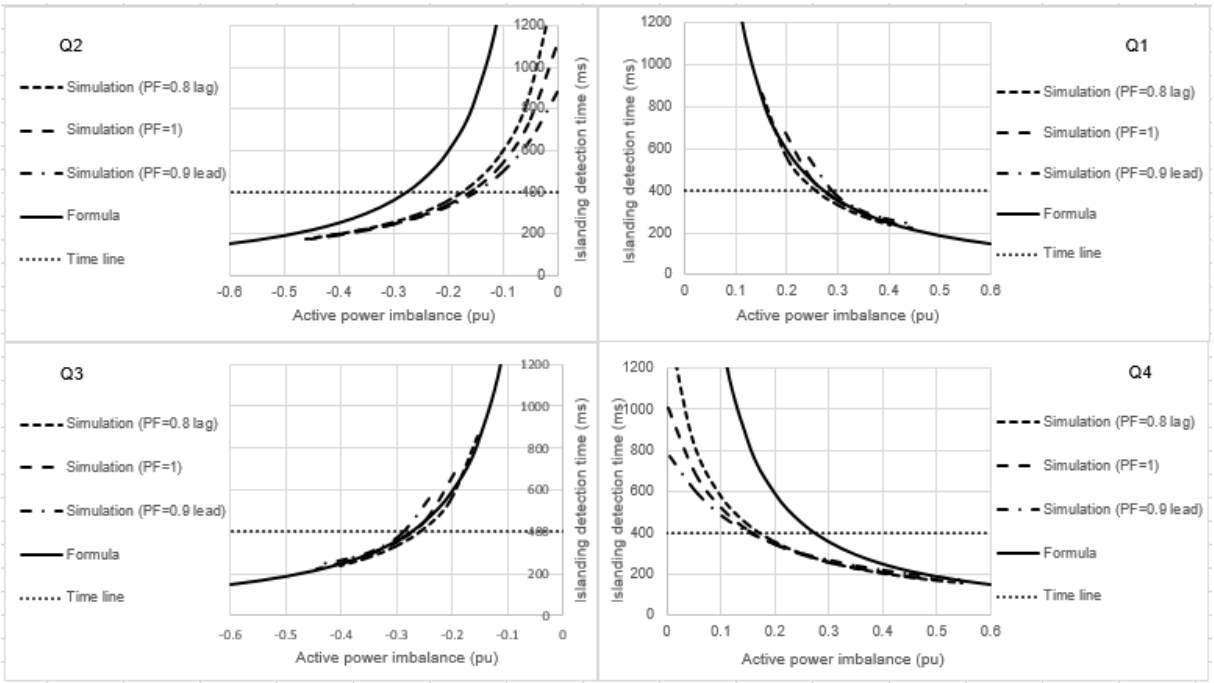

***Figure 4.4**: Impact of operating quadrant on the performance curve of the frequency relay: comparison between simulation curves and formula curve*

A very close match can be seen between the simulation curves and the formula curve in Q1 and Q3. In fact, for an islanding detection time of 400 ms, σ equals 0.013 pu in both quadrants, very close to zero in deed. In contrast σ assimilates a bigger value in Q2 and Q4 (σ = 0.094 pu in both quadrants). This is because the reactive power imbalance which is not taken into account in the formula, has a much bigger influence on the anti-islanding performance of the relay in Q2 and Q4 than it has in Q1 and Q3. This is elucidated in section 4.4.3.

4.4.3 Analysis and interpretation of the results

As seen in Figure 4.3, for excess of active power cases (Q1 and Q4), the relay is more sensitive in Q4 than it is in Q1 while for deficit of active power cases (Q2 and Q3) the relay is more sensitive in Q2 than it is in Q3. Let's consider the performance curve for a load PF of 0.8 lagging for example. For an islanding detection time of 400 ms, the

critical active power imbalances are 0.175 pu in Q4 versus 0.26 pu in Q1 and – 0.17 pu in Q2 versus – 0.253 pu in Q3. The improved performance of the relay in Q2 and Q4 can be verified for other PFs and can be explained by what happens right after islanding.

The deficit of reactive power in Q4 will cause the load voltage and thus the active power consumed by the load to decay after islanding. Since there is excess of active power in this quadrant, this will lead to an even bigger excess of active power, which causes the generator speed, hence the frequency to increase very fast. The result is fast islanding detection.

The situation is very similar in Q2 where the excess of reactive power forces the load voltage to increase after islanding and the load to consume more active power. Since there is already deficit of active power, the increased deficit of active power forces the generator to decelerate fast. The result is a steep decline in island frequency and a fast islanding detection.

In Q1 and Q3 the situation is quite different. In these two quadrants, the active and reactive power imbalances have the same sign (either they are all positive or negative). As a result, the active power imbalance remains small after islanding and the detection time is long.

Therefore, when the island operating point is not known or when it is changing, the setting of the relay must assume operation in Q1 and Q3 since these cases lead to safe solutions.

4.5 Impact of load power factor on the relay performance

4.5.1 Simulation results

Figure 4.5 presents the results of the simulations to evaluate the effect of load PF on the relay anti-islanding performance. The simulations were carried out on a load of 12 MVA considering the PFs shown in the figure. The reactive power imbalance in the island was maintained constant at 0.1 pu in Q1 and – 0.1 pu Q3. The relay frequency and time delay settings were fixed at 51 Hz/ 0 ms in Q1 and 49 Hz/ 0 ms in Q3.

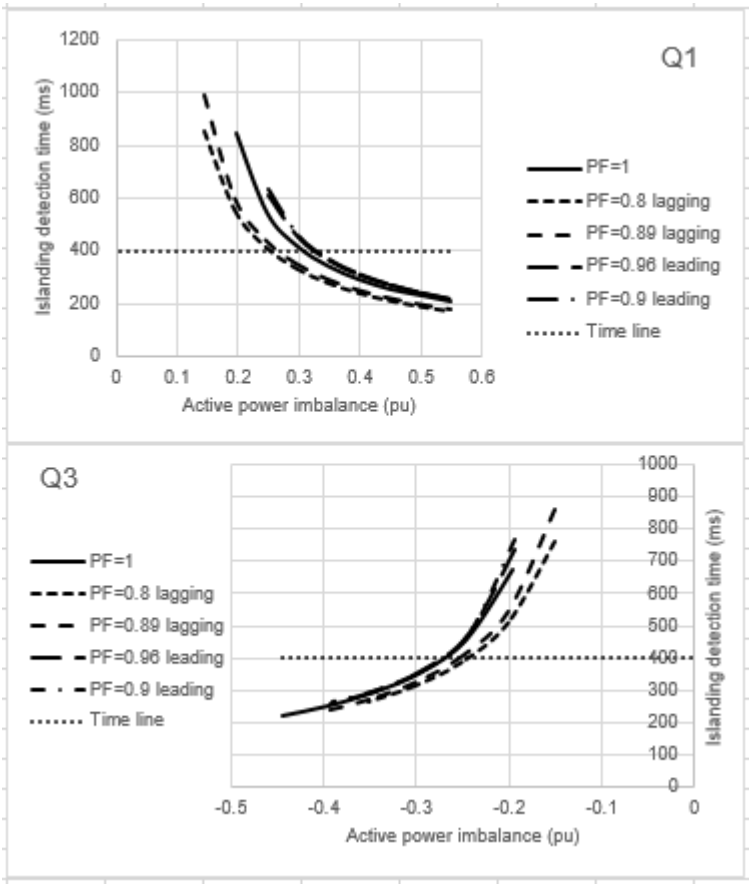

Figure 4.5: *Impact of load PF on the performance curve of the frequency relay*

4.5.2 Validation of the simulation results

The comparison between the simulation curves and the formula curve is shown in Figure 4.6. A close match can be observed between these curves indeed. σ equals 0.018 pu in Q1 and 0.016 pu in Q3.

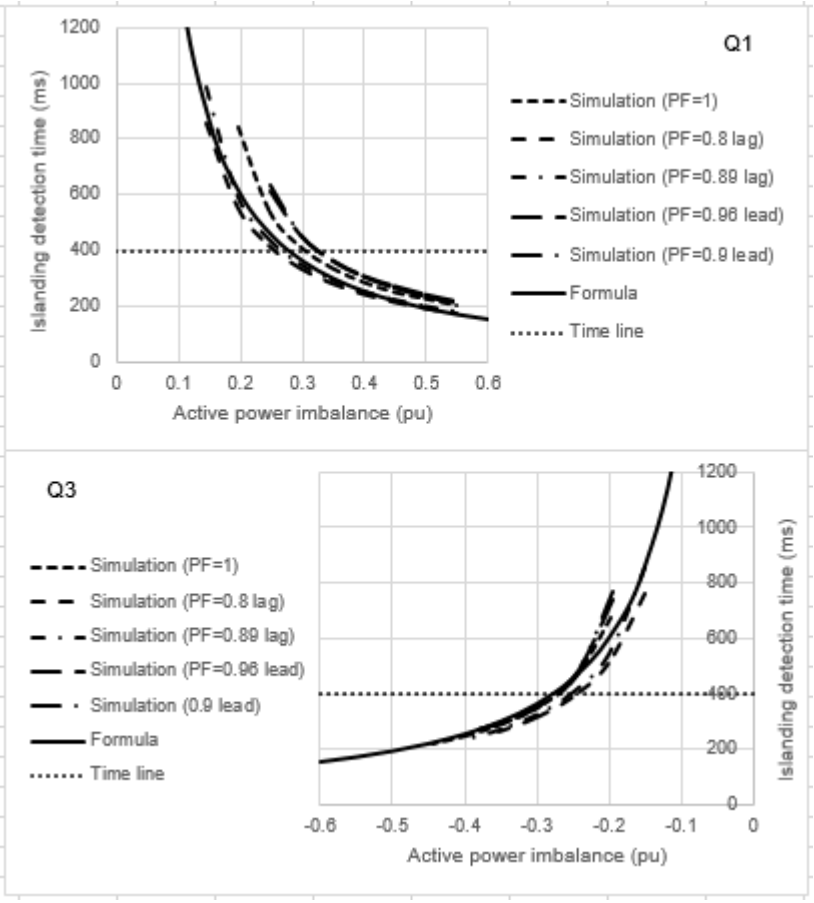

***Figure 4.6**: Impact of load PF on the performance curve of the frequency relay: comparison between simulation curves and formula curve*

4.5.3 Analysis and interpretation of the results

As we can see in Figure 4.5, for a load PF of 0.9 leading and an islanding detection time of 400 ms in Q1, the critical power imbalance is 0.32 pu. It decreases to 0.3 pu for unity PF and is even smaller for lagging PFs. Hence, the safest settings are determined considering the smallest possible leading PF of the local load because it corresponds to the biggest critical power imbalance. However, if the local load cannot operate with leading PFs, then unity PF must be assumed.

Similar conclusions can be drawn for operation in Q3, considering absolute values of power imbalance.

4.6 Impact of reactive power imbalance on the relay performance

4.6.1 Simulation results

Figure 4.7 shows the results of the simulations to study the effect of reactive power imbalance on the relay anti-islanding performance. The simulations were carried out on a load of 12 MW, 0 MVAR (PF = 1) considering different values of reactive power

imbalance. The relay frequency and time delay settings were fixed at 51 Hz/ 0 ms in Q1 and 49 Hz/ 0 ms in Q3.

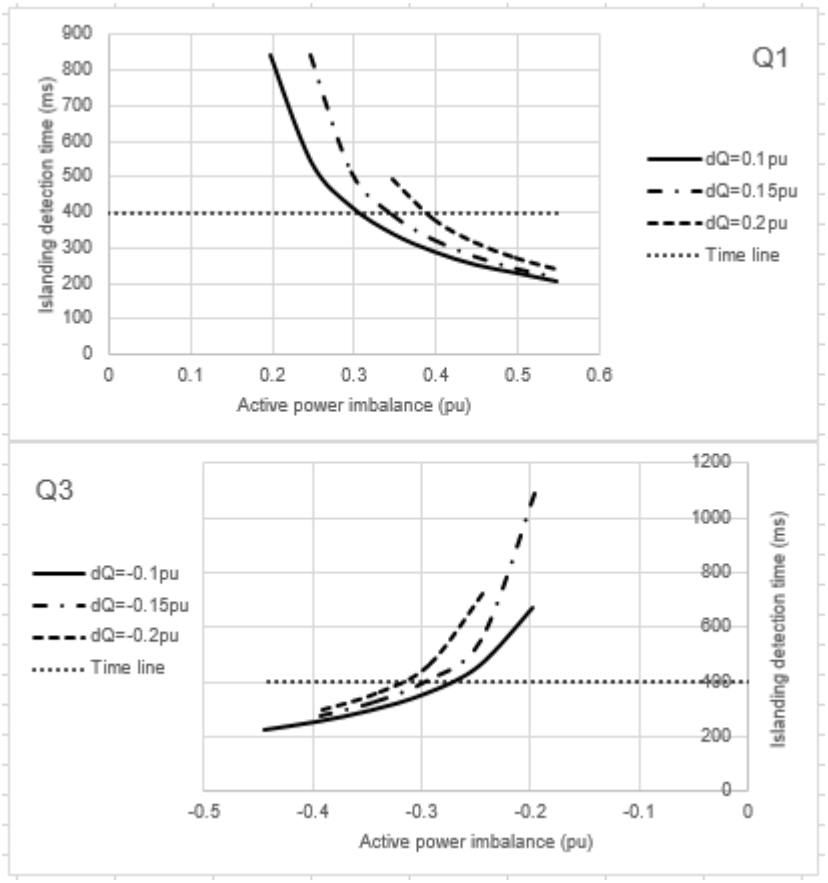

Figure 4.7: *Impact of reactive power imbalance on the performance curve of the frequency relay*

4.6.2 Validation of the simulation results

The comparison between the simulation curves and the formula curve is shown in Figure 4.8. σ equals 0.066 pu in Q1 and 0.026 pu in Q3; very close to zero. Equation (4.1) does not account for the reactive power imbalance in the island. It is for this reason that we observe an increase in the absolute deviation of the active power imbalance (Di), given by equation (4.3), as the reactive power imbalance (absolute value) increases.

$$\mathrm{Di} = |\Delta \mathrm{P_i} - \overline{\Delta \mathrm{P}}| \tag{4.3}$$

In Q1, $\mathrm{D_i}$ takes up the values of 0.025 pu, 0.075 pu, and 0.105 pu for reactive power imbalances of 0.1 pu, 0.15 pu and 0.2 pu respectively and in Q3, $\mathrm{D_i}$ equals 0 pu, 0.025 pu, and 0.045 pu for reactive power imbalances of – 0.1 pu, – 0.15 pu , and – 0.2 pu respectively.

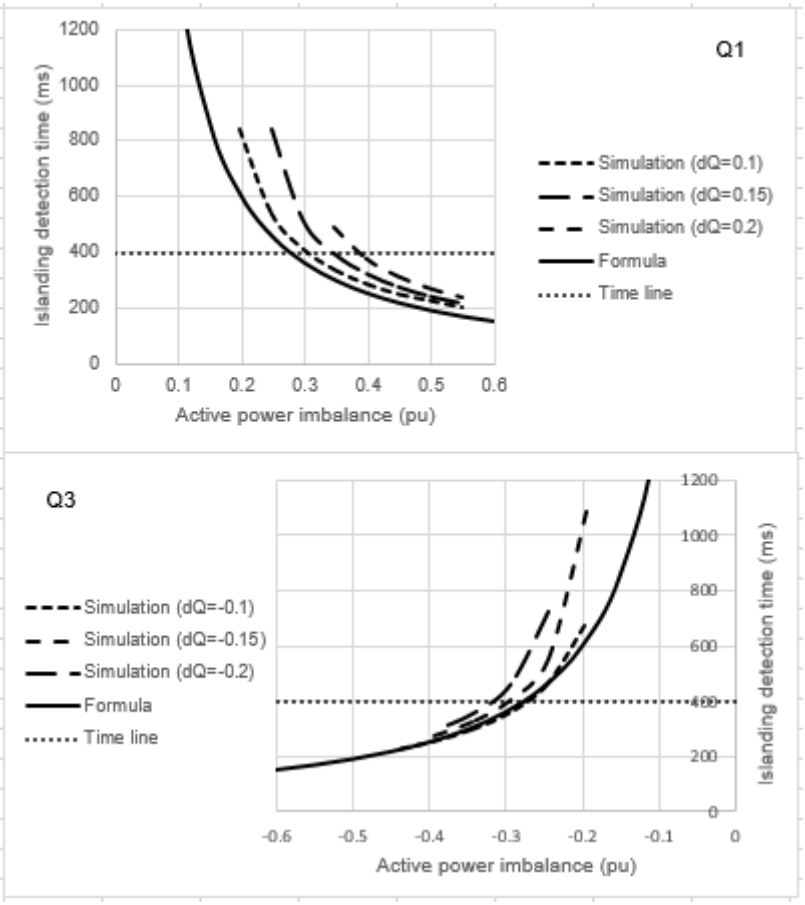

***Figure 4.8**: Impact of reactive power imbalance on the performance curve of the frequency relay: comparison between simulation curves and formula curve*

4.6.3 Analysis and interpretation of the results

It is clear from Figure 4.7 that in both Q1 and Q3, islanding is more difficult to detect with bigger reactive power imbalances (considering absolute values). Let's consider for example an islanding detection time of 400 ms in Q1. The active power imbalances needed to detect islanding are 0.39 pu, 0.35 pu, and 0.3 pu for reactive power imbalances of 0.2 pu, 0.15 pu, and 0.1 pu respectively. Thus if the operating point is not known or if it is changing, the setting of the relay must be based on the highest possible value of the reactive power imbalance in the island.

4.7 Impact of multi-stage tripping on the relay performance

4.7.1 Simulation results

Figure 4.9 shows the results of the simulations to study the effect of multi-stage tripping on the relay anti-islanding performance. The simulations were performed on a load of 12 MW, 0 MVAR (PF = 1) considering the frequency and time delay settings shown in

the figure. The reactive power imbalance was kept constant at 0.1 pu in Q1 and – 0.1 pu in Q3.

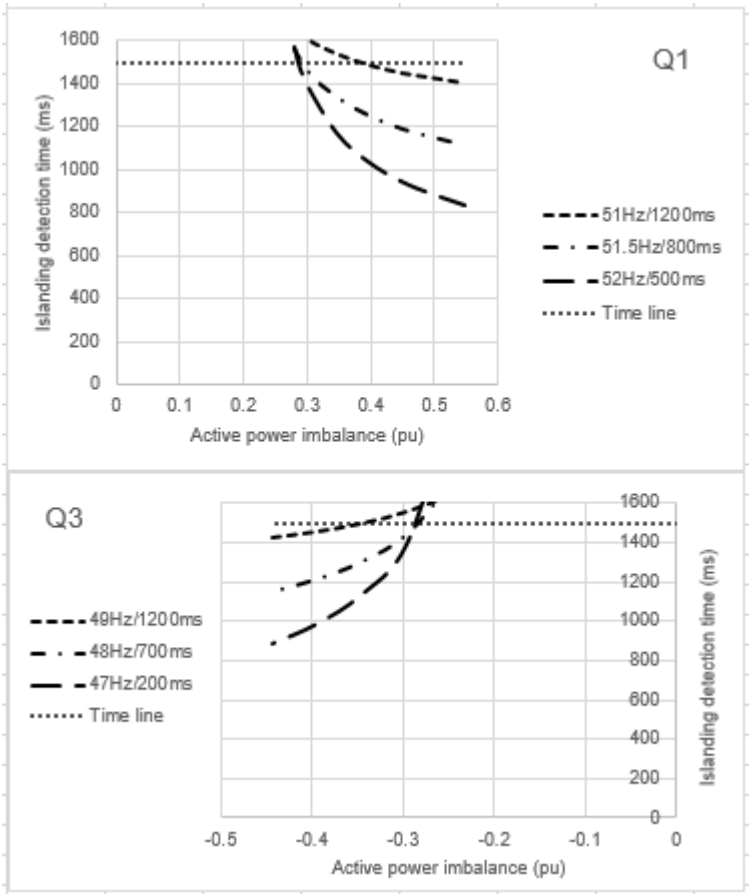

***Figure 4.9**: Impact of multi-stage tripping on the performance curve of the frequency relay*

4.7.2 Validation of the simulation results

The comparison between the simulation curves and the formula curves for multi-stage tripping is shown in Figure 4.10. A close match can be observed between simulation curves and formula curves for the same frequency and time delay settings. For an islanding detection time of 1500 ms in Q1, D_i takes up the values of 0.03 ms, 0.03 ms, and 0.06 ms for relay settings of 51 Hz/ 1200 ms, 51.5 Hz/ 800 ms, and 52 Hz/ 400 ms respectively. The two sets of curves are even more closely matched in Q3 where D_i equals 0.03 ms for 47 Hz/ 200 ms and zero for the other two settings.

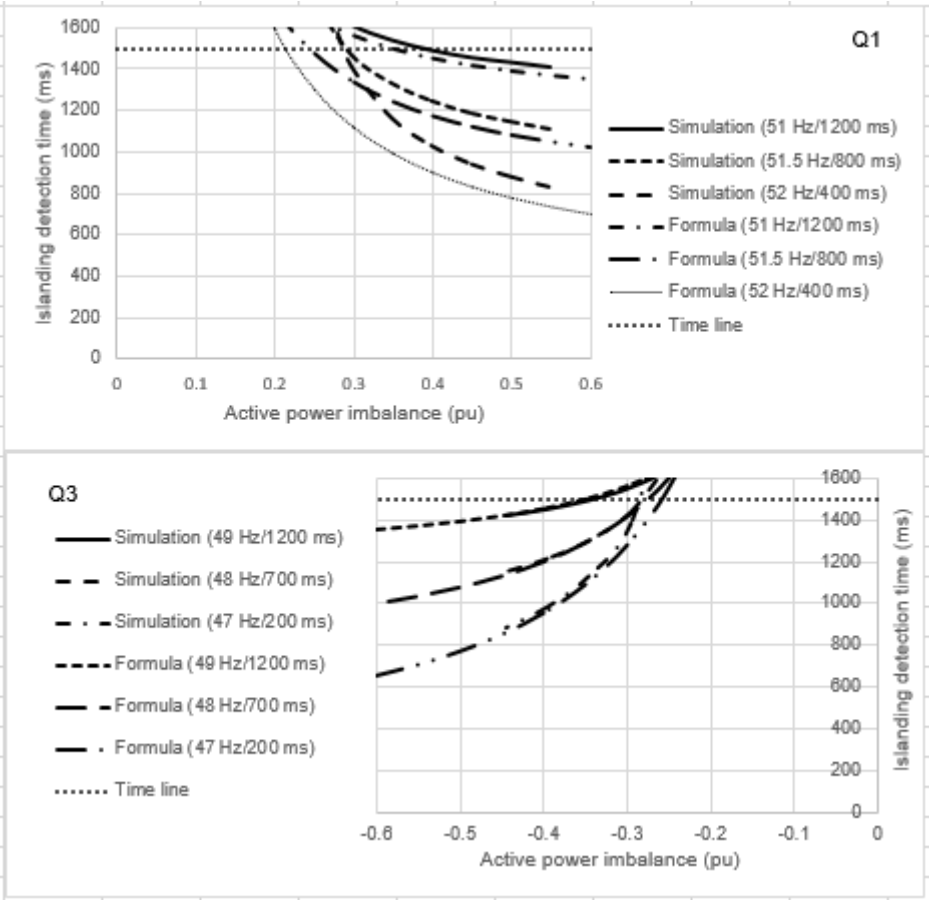

***Figure 4.10**: Impact of multi-stage tripping on the performance curve of the frequency relay: comparison between simulation curves and formula curves*

4.7.3 Analysis and interpretation of the results

We observe in Figure 4.9 that for an islanding detection time of 1500 ms, the active power imbalances necessary to detect islanding in Q1 vary from 0.38 pu for the 51 Hz/ 1200 ms curve to about 0.29 pu for the 51.5 Hz/800 ms curve, and 0.285 pu for the 52 Hz/ 500 ms curve. Particularly for the last two curves, we can see that for longer islanding detection times, multi-stage setting affects the anti-islanding characteristics of the relay very little. Hence, multi-stage tripping can improve the anti-islanding performance of the frequency relay by reducing the active power imbalance required to detect islanding. Similar conclusions may be reached for operation in Q3.

4.8 Guideline for setting the frequency relay

Based on the results of the simulations above, we recommended that the following guideline be adhered to when adjusting the frequency setting and time delay setting of a frequency relay to protect a synchronous distributed generator against islanding and abnormal frequency deviations. Adherence to this guideline will ensure that the relay is adjusted safely at all times.

i) The relay engineer must assume operation in Q1 to determine overfrequency settings and corresponding time delay settings and operation in Q3 to determine underfrequency settings and corresponding time delay settings.

ii) The relay engineer must assume unity load PF.

iii) The relay engineer must consider the biggest possible value of reactive power imbalance (absolute value) that can exist in the island.

iv) The relay engineer must set the relay to trip in multiple stages.

5. Setting the voltage relay

5.1 Introduction

Voltage relays employed for the islanding detection of a synchronous generator must be set so as not to interfere with the normal operation of the network. For that to be possible, the relay's anti-islanding performance curve must present a reactive power imbalance bigger than the critical reactive power imbalance. For a given islanding detection time, the critical reactive power imbalance will be affected by many operating parameters including island operating quadrant, load PF, and active power imbalance in the island. The objective of this chapter is to investigate how these parameters affect the anti-islanding performance curve (and hence the critical reactive power imbalance) of the voltage relay in order to understand how to safely set the relay.

5.2 Simulation procedure

The simulations use the test system of Figure 5.1.

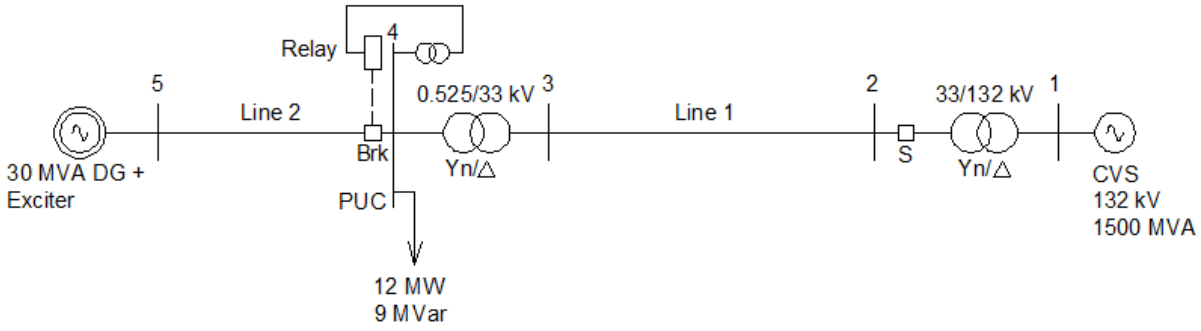

***Figure 5.1**: Schematic of the test system*

The reactive power imbalance in the island is varied from 0 to 1.0 pu in Q1 and Q2 and from 0 to – 1.0 pu in Q3 and Q4 by varying the generator reactive power output. For each reactive power imbalance value, an islanding is simulated by opening switch S. Then the pairs of reactive power imbalance value at bus 4 and relay pickup time are used to plot the performance curve.

5.3 Flowchart of the simulation process

Three groups of simulations (impact of the operating quadrant on the relay performance, impact of load PF on the relay performance, and impact of active power imbalance on the relay performance) are carried out in the following sections, the ultimate objective of each group of simulations being the determination of conditions

in which islanding is hardest to detect. These conditions form the most pessimistic cases of islanding detection and inform the setting of the relay. The flowchart of Figure 5.2 pictures the interaction between these groups.

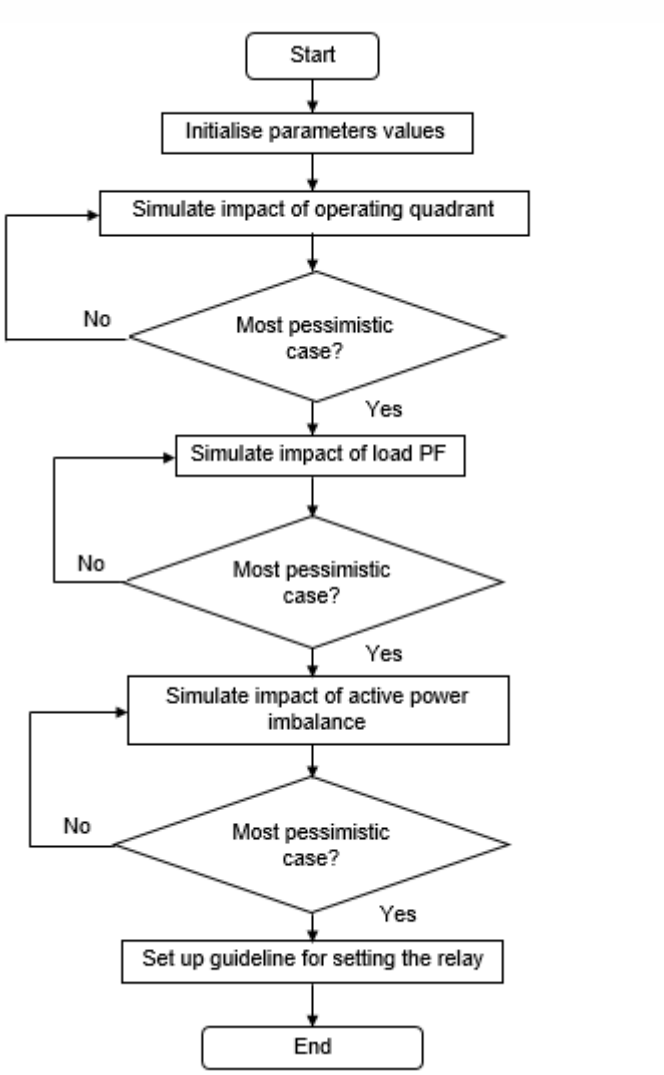

***Figure 5.2**: Flowchart of the simulation process to study the anti-islanding performance of the voltage relay and set up a guideline for adjusting the relay*

5.4 Impact of operating quadrant on the relay performance

5.4.1 Simulation results

Figure 5.3 presents the results of the simulations to evaluate the effect of the operating quadrant on the relay anti-islanding performance. The simulations were carried out on a load of 12 MVA considering different values of load PF. The active power imbalance in the island was maintained constant at 0.0333 pu in Q1 and Q4 and – 0.0333 pu in Q2 and Q3. The relay voltage and time delay settings were fixed at 1.1 pu/ 0 ms in Q1 and Q2 and 0.9 pu/ 0 ms in Q3 and Q4.

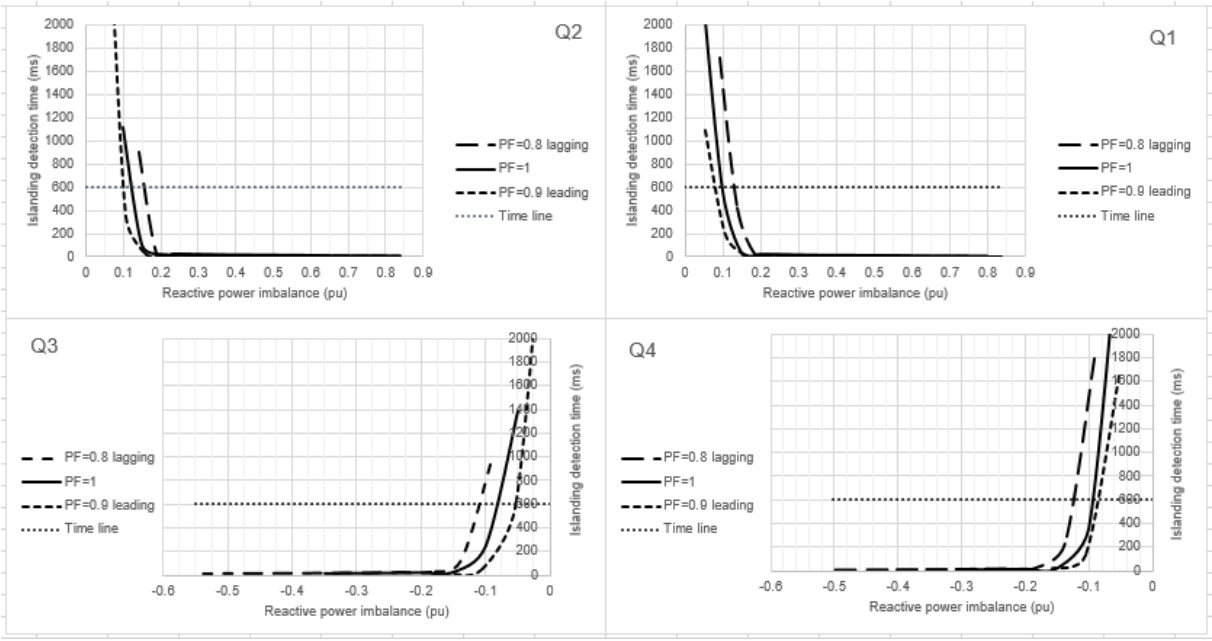

***Figure 5.3**: Impact of island operating quadrant on the performance curve of the voltage relay*

5.4.2 Validation of the simulation results

The simulation curves are validated against the performance curve of a voltage relay operating in similar conditions (Vieira et al, 2007: 489). Let's call the relay against whose performance curve the validation is done, the reference relay. If we consider the reactive power imbalance of this relay ($\overline{\Delta Q}$) for a given islanding detection time (t) as the expected value, then the sample standard deviation (σ) of a sample $\Delta Q_i \ldots \Delta Q_n$ consisting of reactive power imbalances determined by simulation for the same islanding detection time can be calculated in accordance with equation (3.1) as follows:

$$\sigma = \sqrt{\frac{1}{n-1} \sum_{i=1}^{n} (\Delta Q_i - \overline{\Delta Q})^2} \qquad (5.1)$$

The simulation curves and the reference relay's curve are compared in Figure 5.4. For an islanding detection time of 600 ms in Q1 and Q2, a close match can be seen between these curves. σ equals 0.027 pu in Q1 and 0.022 pu in Q2; fairly close to zero. Yet, for an islanding detection time of 10 ms, σ increases drastically (σ = 0.209 pu in Q1 and Q2). This is because the time constant (τ) of the reference circuit (τ = 7.6 ms) is larger than that of the simulation circuit (τ = 4.5 ms). Accordingly, the reference circuit voltage takes longer to change after islanding than the simulation circuit voltage. Similar conclusions apply to Q3 and Q4.

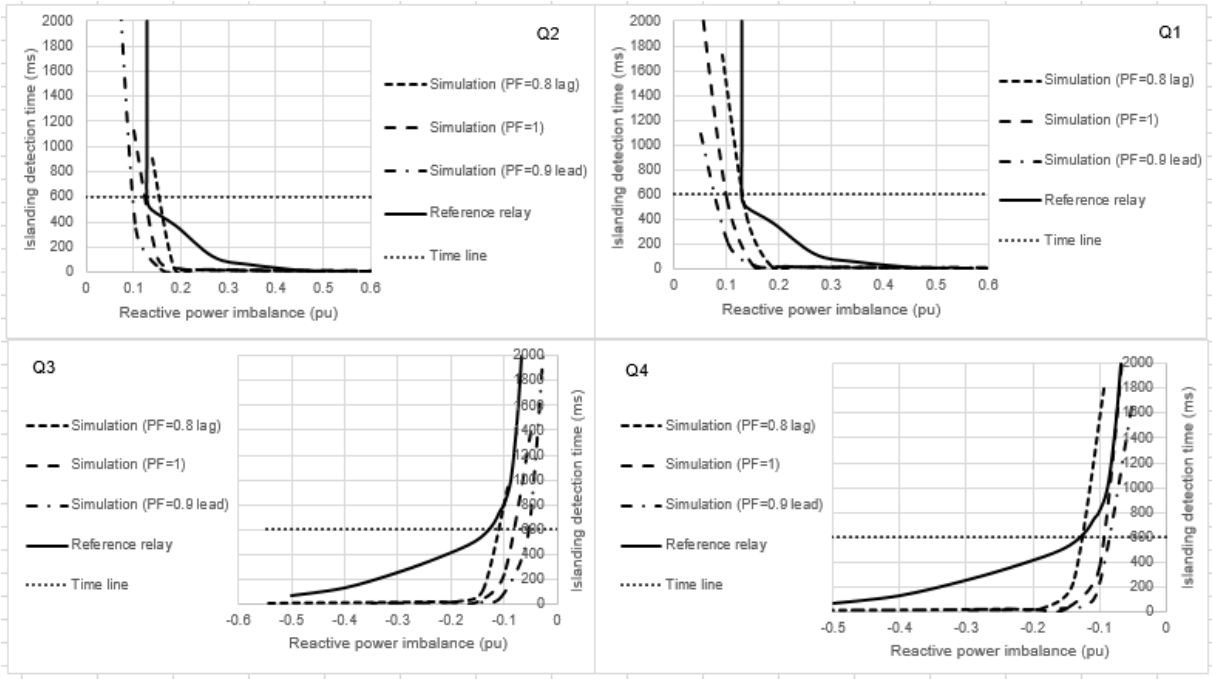

***Figure 5.4**: Impact of operating quadrant on the performance curve of the voltage relay: comparison between simulation curves and reference curve*

5.4.3 Analysis and interpretation of the results

Figure 5.3 demonstrate that the ability of the voltage relay to detect islanding depends on the combination of active and reactive power imbalances in the island. We can see that for excess of reactive power cases (Q1 and Q2), the relay is more sensitive in Q1 than it is in Q2 while for deficit of reactive power cases (Q3 and Q4) the relay is more sensitive in Q3 than it is in Q4. Let's consider for example the performance curve for a load PF of 0.9 leading. For an islanding detection time of 600 ms, the reactive power imbalances are 0.08 pu in Q1 versus 0.1 pu in Q2 and 0.055 pu in Q3 versus 0.0875 pu in Q4. Therefore, when the operating point is not known or when it is changing, the setting of the relay must assume operation in Q2 and Q4 because these cases lead to safe solutions.

5.5 Impact of load power factor on the relay performance

5.5.1 Simulation results

Figure 5.5 presents the results of the simulations to evaluate the effect of load PF on the relay anti-islanding performance. The simulations were carried out on a load of 12 MVA considering the values of load PF shown in the figure. The active power imbalance in the island was maintained constant at – 0.0333 pu in Q2 and 0.0333 pu

in Q4. The relay voltage and time delay settings were fixed at 1.1 pu/ 0 ms in Q2 and 0.9 pu/ 0 ms in Q4.

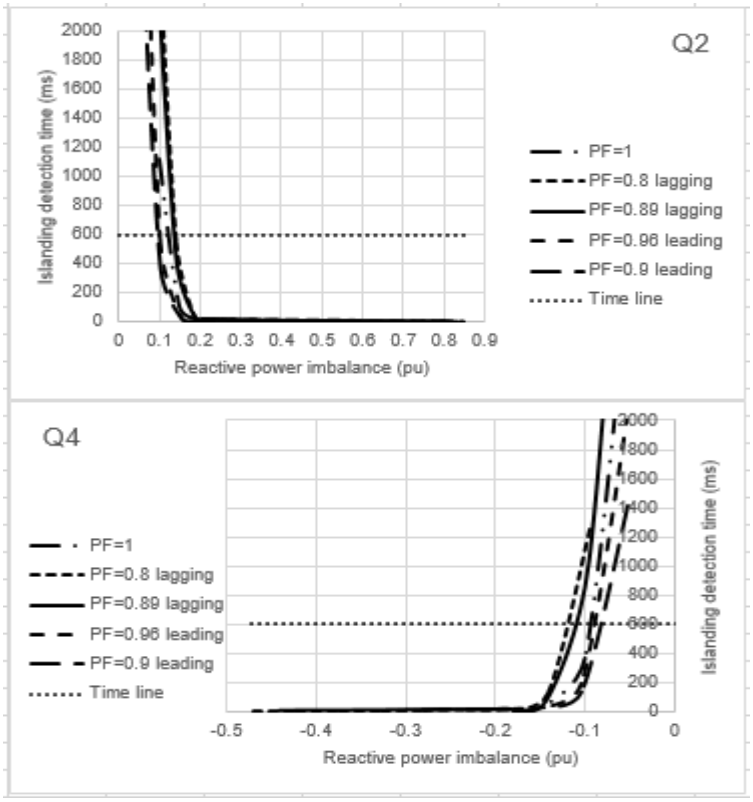

Figure 5.5: *Impact of load PF on the performance curve of the voltage relay*

5.5.2 Validation of the simulation results

The comparison between the simulation curves and the reference curve is shown in Figure 5.6. σ equals 0.022 pu in Q2 for an islanding detection time of 600 ms and 0.209 pu for an islanding detection time of 10 ms. As explained above, the difference in time constants is the reason for the increased σ near zero ms. In Q4, σ equals 0.013 pu for 600 ms and 0.209 pu for 90 ms.

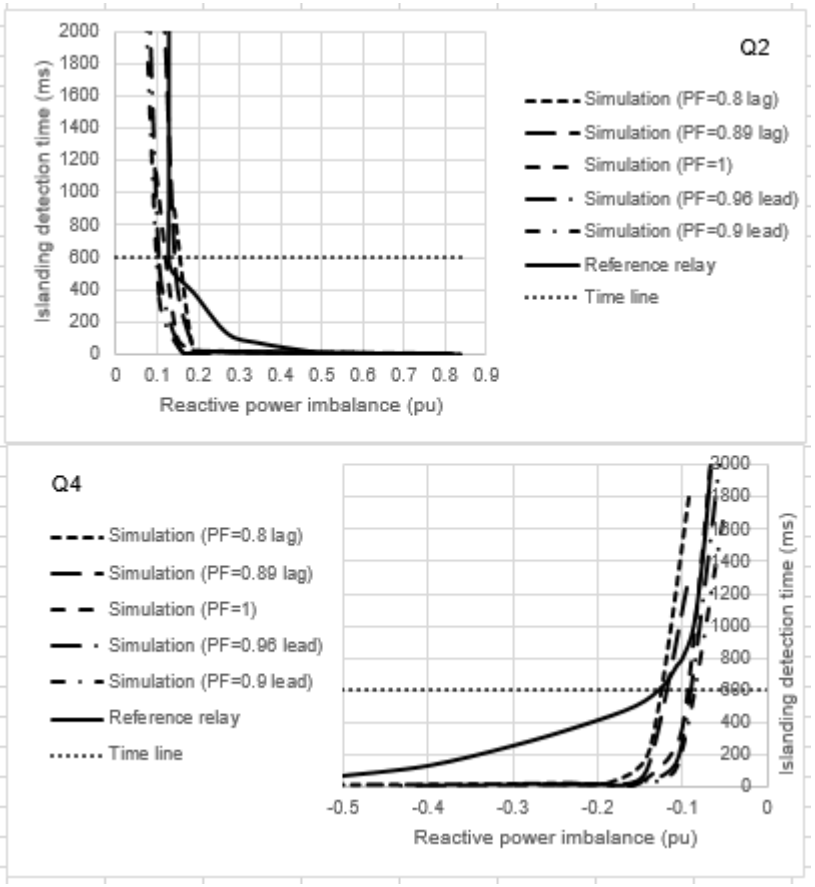

***Figure 5.6**: Impact of load PF on the performance curve of the voltage relay: comparison between simulation curves and reference curve*

5.5.3 Analysis and interpretation of results

In Q2, Figure 5.5, load PF affects the performance curve on a very narrow range of reactive power imbalance. Above 0.2 pu, load PF has no effect on the performance curve as islanding is detected almost immediately no matter the load PF. However, between 0.05 pu and 0.2 pu, load PF affects the performance curve considerably. For example, for an islanding detection time of 600 ms, a reactive power imbalance of about 0.15 pu is required to detect islanding when the load PF is 0.8 lagging. The value decreases to about 0.12 pu for unity PF and is even smaller for leading PFs. Hence, the setting of the relay must be based on the smallest possible value of load lagging PF because this represents the condition in which islanding is hardest to detect.

Similar conclusions can be reached for operation in Q4, considering absolute values of reactive power imbalance.

5.6 Impact of active power imbalance on the relay performance

5.6.1 Simulation results

Figure 5.7 presents the results of the simulations to study the effect of active power imbalance on the relay anti-islanding performance. The simulations were carried out on a load of 12 MW, 0 MVAR (PF = 1). The active power imbalance in the island was varied to study its effect on the performance curve. The relay voltage and time delay settings were fixed at 1.1 pu/ 0 ms in Q2 and 0.9 pu/ 0 ms in Q4.

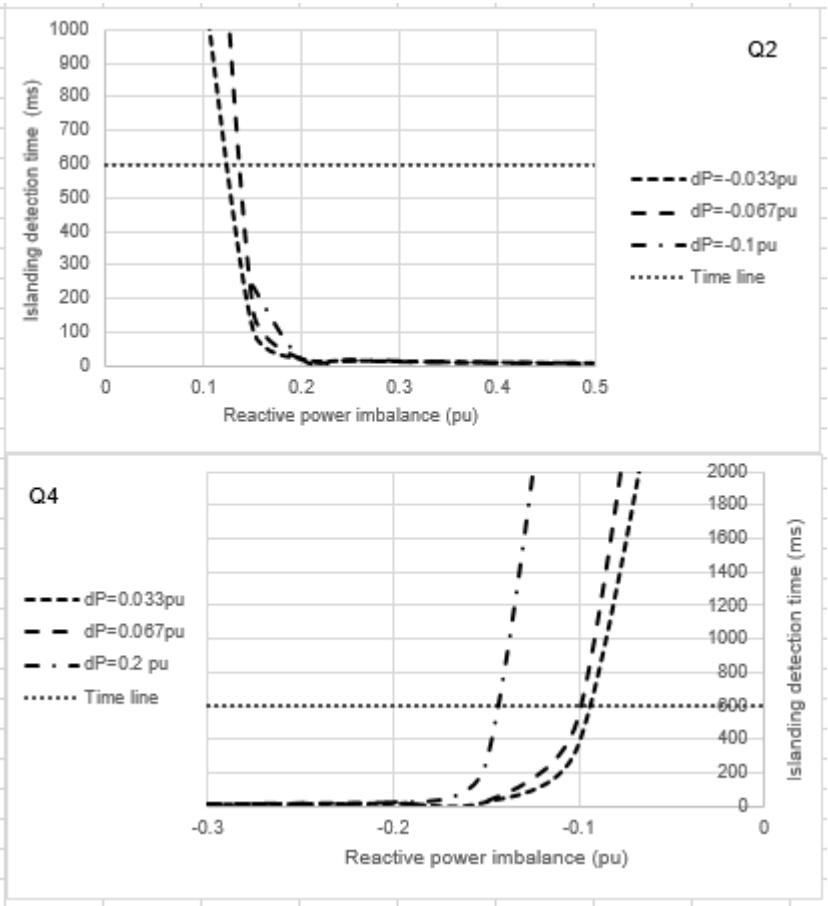

Figure 5.7: *Impact of active power imbalance on the performance curve of the voltage relay*

5.6.2 Validation of the simulation results

The comparison between simulation curves and the reference curve is shown in Figure 5.8.In Q2, σ is close to zero for an islanding detection time of 600 ms and 0.209 pu for 10 ms. As explained above, the difference in time constants is the reason for the increased σ near zero. In Q4, σ = 0.023 pu for 600 ms and 0.307 pu for 90 ms.

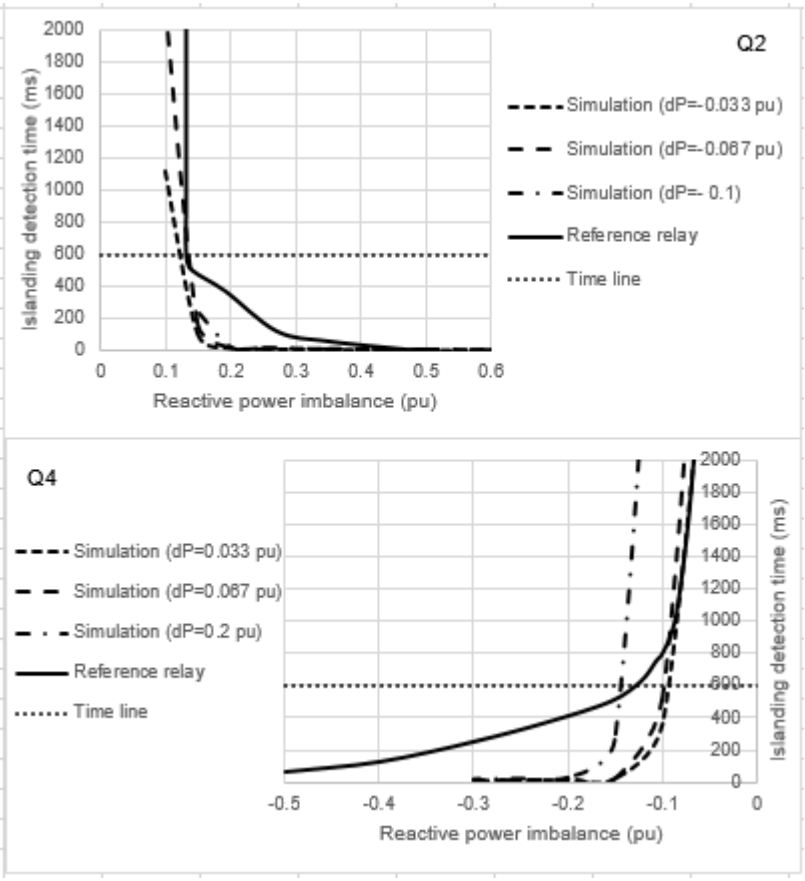

Figure 5.8*: Impact of active power imbalance on the performance curve of the voltage relay: comparison between simulation curves and reference curve*

5.6.3 Analysis and interpretation of the results

In Q4, Figure 5.7, islanding becomes more difficult to detect with bigger active power imbalances. In fact, with a reactive power imbalance of – 0.15 pu, islanding would be detected in 50 ms if the active power imbalance was 0.067 pu while it would take up 300ms to detect if the active power imbalance was 0.333 pu. Thus if the operating point is not known or if it is changing, the relay setting must be based on the highest possible value of active power imbalance that can exist in the island.

Similar conclusions can be drawn for operation in Q2, considering absolute values of active power imbalance. However, the range of possible active power imbalances in this quadrant is very limited by network operating constraints.

5.7 Guideline for setting the voltage relay

Based on the results of the simulations above, we recommended that the following guideline be adhered to when adjusting the voltage setting and time delay setting of a voltage relay to protect a synchronous distributed generator against islanding and

abnormal voltage deviations. Adherence to this guideline will ensure that the relay is adjusted safely at all times.

i) The relay engineer must assume operation in Q2 to determine the overvoltage settings and corresponding time delay settings and operation in Q4 to determine the undervoltage settings and corresponding time delay settings.

ii) The relay engineer must consider the smallest possible value of load lagging PF.

iii) The relay engineer must assume the highest possible value of active power imbalance (absolute value) that can exist in the island.

6. Conclusion and future work

6.1 General discussion

Distribution networks are designed for unidirectional power flow from the substation at high voltage level to consumers at low voltage level. The introduction of a generator on the distribution line (such a generator is called distributed generator) poses protection problems. Islanding is one of them.

Islanding occurs when the generator continues to supply loads after the disconnection of the grid. Islanding poses a problem of safety, power quality, and risk of asynchronous reclosing. The solution to islanding is to disconnect the generator soon after it occurs. Many algorithms exist but the frequency relay and the voltage relay have attracted a lot of interest because of their simplicity and the need to avoid false tripping, a weak point of anti-islanding relays.

When employed for islanding detection, the frequency relay must satisfy the islanding detection requirement (maximum time to detect islanding) and the frequency variation immunity requirement (range of frequency variation for which the generator is required to remain connected to the network and uphold normal operation). These two requirements are conflicting because when the relay is set sensitive enough to detect islanding, it might interfere with the normal operation of the generator, and when it is set less sensitive to satisfy the frequency variation immunity requirement, it might not detect islanding timeously.

This conflict is solved by determining the critical active power imbalance of the relay in the islanding detection time versus active power imbalance graph. In order to satisfy the islanding detection requirement and the frequency variation immunity requirement simultaneously, the relay performance curve must present an active power imbalance bigger than the critical active power imbalance (considering absolute values).

Similarly, to satisfy the islanding detection requirement and the voltage variation immunity requirement simultaneously, the voltage relay performance curve must present a reactive power imbalance bigger than the critical reactive power imbalance (considering absolute values).

The aim of this dissertation was to investigate the effect of the following parameters on the anti-islanding performance characteristics of the frequency relay and the implication for the relay setting: island operating quadrant, load power factor, and reactive power imbalance. It was found that islanding was hardest to detect in Q1 (excess of active power and reactive power) and Q3 (deficit of active power and reactive power) and for the following operating conditions: smallest leading power factor, and biggest reactive power imbalance (absolute value).

In respect to the voltage relay, the aim was to investigate the effect of the operating quadrant, load power factor, and active power imbalance on the performance curve and the implication for the relay setting. It was found that the voltage relay struggles to detect islanding in Q2 (deficit of active power and excess of reactive power) and Q4 (excess of active power and deficit of reactive power) and for the following operating conditions: smallest lagging load power factor and biggest active power imbalance (absolute value).

The dissertation also investigated the effect of multi-stage setting on the anti-islanding performance of the frequency relay. It was found that multi-stage setting improves the anti-islanding ability of the frequency relay by reducing the active power imbalance required to detect islanding.

6.2 Conclusions

To adjust the frequency relay to satisfy both the anti-islanding requirement and the frequency variation immunity requirement:

i) The relay engineer must assume operation in Q1 to determine overfrequency settings and corresponding time delay settings and operation in Q3 to determine underfrequency settings and corresponding time delay settings.

ii) The relay engineer must consider the biggest possible value of reactive power imbalance (absolute value) that can exist in the island.

iii) The relay engineer must assume unity load PF.

To adjust the voltage relay to satisfy both the anti-islanding requirement and the voltage variation immunity requirement:

i) The relay engineer must assume operation in Q2 to determine overvoltage settings and corresponding time delay settings and operation in Q4 to determine undervoltage settings and corresponding time delay settings.

ii) The relay engineer must consider the smallest possible value of load lagging PF.

iii) The relay engineer must assume the highest possible value of active power imbalance (absolute value) that can exist in the island.

6.3 Future work

There are many modes of control of the synchronous generator but often, it operates in reactive power control mode or in voltage control mode. Here we have investigated the impact of island operating quadrant, load PF and reactive power imbalance on the anti-islanding performance characteristics of the frequency relay with a generator operating in reactive power control mode. A similar study can be conducted with a generator operating in voltage control mode.

Bibliography

ACKERMANN, T., ANDERSSON, G. and SÖDER, L., 2001. Distributed generation: a definition. *Electric Power Systems Research,* **57**(3), pp. 195-204.

AFFONSO, C., FREITAS, W., XU, W. and DA SILVA, L., 2005. Performance of ROCOF relays for embedded generation applications. *IEE Proceedings-Generation, Transmission and Distribution,* **152**(1), pp. 109-114.

CARLEY, S., 2009. Distributed generation: An empirical analysis of primary motivators. *Energy Policy,* **37**(5), pp. 1648-1659.

BRIGHT, C., 2001. COROCOF: comparison of rate of change of frequency protection. A solution to the detection of loss of mains, *Developments in Power System Protection, 2001, Seventh International Conference on (IEE)* 2001, IET, pp. 70-73.

DRIESEN, J. and BELMANS, R., 2006. Distributed generation: challenges and possible solutions, *Power Engineering Society General Meeting, 2006. IEEE* 2006, IEEE, pp. 8 pp.

FREITAS, W. and XU, W., 2004. False operation of vector surge relays. *IEEE Transactions on Power Delivery,* **19**(1), pp. 436-438.

FREITAS, W., XU, W., AFFONSO, C.M. and HUANG, Z., 2005. Comparative analysis between ROCOF and vector surge relays for distributed generation applications. *IEEE Transactions on Power Delivery,* **20**(2), pp. 1315-1324.

FREITAS, W., XU, W., HUANG, Z. and VIEIRA, J., 2007. Characteristics of vector surge relays for distributed synchronous generator protection. *Electric Power Systems Research,* **77**(2), pp. 170-180.

GEIDL, M., 2005. *Protection of power systems with distributed generation: state of the art.* ETH, Eidgenössische Technische Hochschule Zürich, EEH Power Systems Laboratory.

GLOVER, J.D., SARMA, M. and OVERBYE, T., 2011. *Power System Analysis & Design, SI Version.* Cengage Learning.

GRAINGER, J.J. and STEVENSON, W.D., 1994. *Power system analysis.* McGraw-Hill New York.

GRUBB, M. and VIGOTTI, R., 1995. *Renewable Energy Strategies for Europe: Electricity systems and primary electricity sources.* Earthscan.

IEEE, 1993. Load representation for dynamic performance analysis. *IEEE Transactions on Power Systems*, **8**(2), pp. 472 – 482.

IEEE, 2003. Standard for interconnecting distributed resources with electric power systems: IEEE standard 1547 – 2003. *IEEE*.

IEEE, 2006. Recommended practice for excitation system models for system stability studies: IEEE Standard 421.5 – 2005. *IEEE.*

IPCC, 2011. Press release: Potential of renewable energy outlined in report by the intergovernmental panel on climate change. Intergovernmental Panel on Climate Change. Available at: http://srren.ipcc-wg3.de/press/content/potential-of-renewable-energy-outlined-report-by-the-intergovernmental-panel-on-climate-change

JENKINS, N., ALLAN, R., CROSSLEY, P., KIRSCHEN, D. and STRBAC, G., 2000. *Embedded generation,* 1st ed. Bristol, UK: Inst. Elec. Eng.

KUNDUR, P., BALU, N.J. and LAUBY, M.G., 1994. *Power system stability and control.* McGraw-Hill, New York.

LOPES, J.P., HATZIARGYRIOU, N., MUTALE, J., DJAPIC, P. and JENKINS, N., 2007. Integrating distributed generation into electric power systems: A review of drivers, challenges and opportunities. *Electric Power Systems Research,* **77**(9), pp. 1189-1203.

NERSA, 2012. Grid connection code requirements for renewable power plants connected to the transmission system or distribution system in South Africa. Draft version 2.1

O'KANE, P. and FOX, B., 1997. Loss of mains detection for embedded generation by system impedance monitoring, *Developments in Power System Protection, Sixth International Conference on (Conf. Publ. No. 434)* 1997, IET, pp. 95-98.

SALMAN, S., KING, D. and WELLER, G., 2001. New loss of mains detection algorithm for embedded generation using rate of change of voltage and changes in power factors, *Developments in Power System Protection, 2001, Seventh International Conference on (IEE)* 2001, IET, pp. 82-85.

STOFT, S., 2002. *Power system economics: Designing markets for electricity*. Wiley, New York.

US DEPARTMENT OF ENERGY, 2010. *2009 Renewable energy data book*. US Department of Energy, New York.

VIEIRA, J., CORREA, D., FREITAS, W. and XU, W., 2005. Performance curves of voltage relays for islanding detection of distributed generators. *IEEE Transactions on Power Systems,* **20**(3), pp. 1660-1662.

VIEIRA, J.C.M., FREITAS, W., XU, W. and MORELATO, A., 2006. Performance of frequency relays for distributed generation protection. *IEEE Transactions on Power Delivery,* **21**(3), pp. 1120-1127.

VIEIRA, J., FREITAS, W. and SALLES, D., 2007. Characteristics of voltage relays for embedded synchronous generators protection. *Generation, Transmission & Distribution, IET,* **1**(3), pp. 484-491.

VIEIRA, J.C.M., FREITAS, W., XU, W. and MORELATO, A., 2008. An investigation on the nondetection zones of synchronous distributed generation anti-islanding protection. *IEEE Transactions on Power Delivery,* **23**(2), pp. 593-600.